



Influence of Axial Restraint and Fire Exposure Scenarios on the Fire Resistance of One-Way Reinforced Concrete Slabs

Fidan Salihu ¹ , Anita Gjukaj ^{1*}, Guxim Rrudhani ¹, Fatos Pllana ¹, Meri Cvetkovska ² 

¹ Faculty of Civil Engineering, University of Pristina "Hasan Prishtina", Pristina 10000, Kosovo.

² Faculty of Civil Engineering, University "Ss. Cyril and Methodius", Skopje 1000, North Macedonia.

Received 03 January 2025; Revised 09 March 2025; Accepted 15 March 2025; Published 01 April 2025

Abstract

This study investigates the behavior of one-way simply supported reinforced concrete slabs under fire conditions, focusing on the effects of axial restraint and fire exposure scenarios on their fire resistance. The slabs are subjected to standard ISO 834 fire exposure, and the nonlinear analysis is carried out via the SAFIR2016 computer program, which employs the finite element method. A comparison of the numerical results with experimental results from various studies has shown good agreement. To verify the reliability of the numerical results, it is essential that the test parameters match those used in the simulations. This study aims to evaluate the accuracy and reliability of fire safety regulations for designing one-way simply supported slabs and to identify potential discrepancies between design codes and numerical findings. A 3D analysis is performed, with discretization using shell elements. The results reveal that axial restraint significantly influences the fire resistance of slabs. When axially restrained and exposed to fire from the bottom, the slab achieves fire resistance exceeding ten hours. However, under the same boundary conditions, the fire resistance of the slab is 339 minutes if the fire acts from the top. Without axial restraint, the direction of fire exposure becomes critical. When the fire acts from the bottom, the primary reinforcement is exposed to high temperatures, causing the slab to lose stability as the resisting moment decreases than the acting moment. Conversely, when the fire acts from the top, the slab without axial restraint shows high fire resistance, as the reinforcement remains in the cooler zone, leading to a fire resistance greater than ten hours.

Keywords: One-Way RC Slab; Axial Restraint; Fire Scenario; Fire Resistance; 3D Analysis; SAFIR2016.

1. Introduction

The design of fire-safe structures requires that the structural elements show resistance when exposed to high temperatures from fire. The load-bearing capacity, functionality, and durability of a building are ensured when floor slabs are designed, taking into account high temperatures in the event of fire. Proper selection and design of these slabs, considering various loads (primarily permanent and variable), are essential for maintaining a stable and safe structure throughout its service life. During a fire, floor slabs do more than just bear loads; they often also function as fire compartment barriers. When compartmentation is necessary, the elements that define the fire compartment boundaries, including joints, must be designed and constructed to maintain their separation function during the specified fire exposure [1]. This design ensures that integrity and insulation failures are prevented and that thermal radiation from the unexposed side is minimized.

The ability of a floor structure to meet fire resistance criteria depends on several factors, including the material's mechanical and thermal properties, initial loading level, support conditions, cross-sectional dimensions, steel ratio,

* Corresponding author: anita.gjukaj@uni-pr.edu

 <http://dx.doi.org/10.28991/CEJ-2025-011-04-03>



concrete cover thickness, and specific fire scenario. Each factor impacts the floor's ability to withstand fire and maintain its performance during and after a fire event.

A durable structure must satisfy the requirements for serviceability, strength, and stability throughout its design life without experiencing significant utility loss or requiring excessive unforeseen maintenance. Research from numerous fire tests and numerical analyses indicates that the failure of a floor structure is often accompanied by significant deformation (deflection). When a structure is near its limit state, residual deflections after a fire can be so severe that the floor may not be usable without extensive rehabilitation. The fire conditions should limit the deflection of the slab to a prescribed value to mitigate this. In accordance with ISO standards [2], this limit is set at $L/30$, where L represents the span of the slab [3-7].

Over the years, there has been extensive growth in the literature concerning the fire behavior of reinforced concrete slabs. Lim & Wade [8] investigated fire-exposed floor slabs, primarily focusing on the impact of compressive membrane action in one-way slabs. They concluded that the behavior of one-way RC slabs during a fire mostly depends on the support conditions and the degree of axial restraint. Allam et al. [9] investigated the fire resistance of one-way simply supported slabs via numerical finite difference analysis. Qiu et al. [10] researched the scale fire test and fire resistance of the one-way slab of a metro. Al-Rousan [11] investigated one-way RC slabs analytically via ANSYS with respect to the time to failure and the physical changes associated with exposure to failure. Salihu et al. [12] studied the resistance of two-way RC slabs under fire exposure via SAFIR software and verified that this software yields satisfactory results in terms of the behavior of these slabs under fire conditions.

Rasheed & Mohammed [13] analyzed the fire resistance of one-way RC slabs reinforced with a combination of steel and glass fiber-reinforced polymer (GFRP) bars. The distance from the fire exposed face of the replaced GFRP bars plays a crucial role. Placing GFRP more centrally and away from the ends has a positive impact, resulting in higher fire resistance performance. Qiu et al. [10] proposed a scaled fire test method to evaluate the fire resistance of large one-way slabs used in metro systems. The theoretical calculation results match the fire test results, and the temperature of the longitudinal rebars at the bottom of the slab is the key factor affecting the fire resistance limit. Increasing the depth of the concrete cover can effectively increase the fire resistance limit.

Kodur et al. [14] studied the fire resistance of concrete slabs incorporating natural fiber-reinforced polymers. The results of this study indicate that bio-based FRP-strengthened RC members undergo faster degradation in terms of moment capacity, experience greater deflections under fire exposure, and exhibit lower fire resistance than do slabs strengthened with conventional FRPs. Elwakkad [15] experimentally studied the behavior of reinforced self-curing concrete slabs exposed to 600°C , which were heated under tension. He concluded that the steel reinforcement ratio has a substantial effect on improving the crack load and ultimate failure load of reinforced self-curing concrete flat slabs. Shhabat et al. [16] experimentally and analytically studied the use of CFRP materials for repairing a reinforced concrete one-way solid slab exposed to thermal shock. They revealed that there was a decrease of approximately 45.4% in the compressive strength of concrete after exposure to thermal shock.

These studies offer valuable insights into how reinforced concrete slabs behave in fires. However, further research is needed to explore how specific parameters affect the fire resistance of one-way RC slabs to understand their performance when exposed to fire conditions and to create more efficient fire protection strategies. Our research addresses several previously overlooked parameters to accurately depict reinforced concrete slab behavior during fire incidents. In addition, numerical 3D simulations were performed via SAFIR2016 to assess the degree to which different parameters—the axial restraint fire scenario—affect the fire resistance of one-way supported reinforced concrete slabs.

To determine how each of the abovementioned parameters affects the fire resistance of one-way simply supported reinforced concrete slabs, only the corresponding parameter is varied; therefore, in each case, a reinforcement equal to the minimum required is adopted. This means that when the reinforcement is adopted, the dimensions of the reinforcement bars that actually exist are not considered. On the basis of the numerically achieved results, certain conclusions that can be useful for meeting the prescribed fire resistance criteria for these types of floor structures are given. This insight can help create more effective fire protection strategies for these structures.

The paper contains 6 sections. The first section presents the introduction, which reviews the published literature and identifies the gaps in the literature. In the second section, the research methodology is presented through a graph. In the third section, numerical modeling for the analysis is described via SAFIR2016 software. In the fourth section, via experiments reported in the literature, the numerical modeling was validated via SAFIR2016 software. The results and discussion are given in the fifth section, and the conclusions of the paper are summarized in the sixth section.

2. Research Methodology

Initially, the literature was reviewed to identify and categorize key findings, methodologies, and limitations. The results of the numerical analyses were subsequently compared with the experimental data reported in the literature. The two sets of results from the fire test showed a satisfactory level of agreement. A parametric analysis was then carried out to assess the fire resistance of one-way reinforced concrete slabs. The effects of axial restraint and fire scenarios were analyzed via numerical 3D analysis in SAFIR2016. Finally, the conclusions of the research are summarized, and the research methodology flowchart is presented in Figure 1.

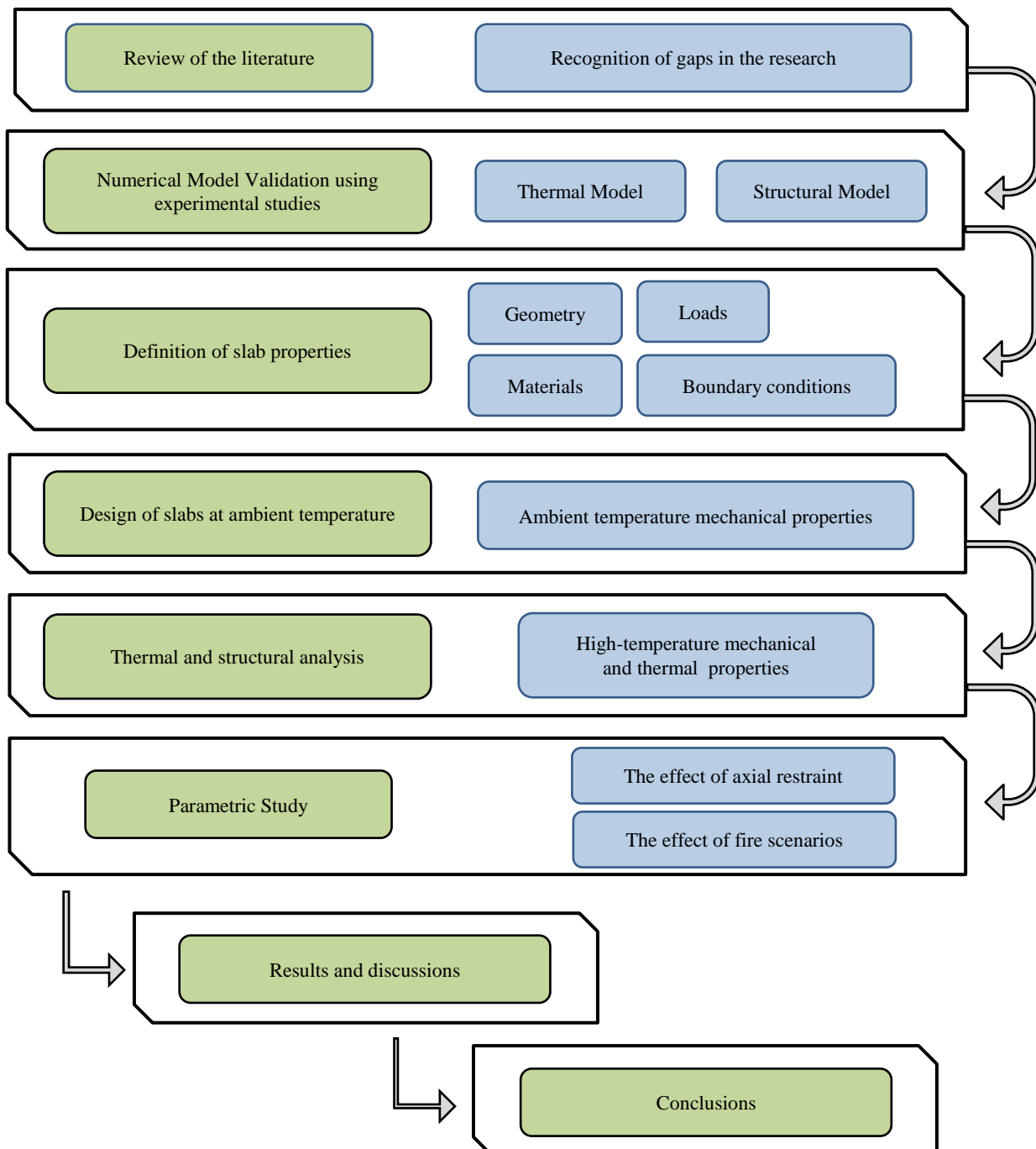


Figure 1. The considered methodology

3. Numerical Model

The concrete and steel constitutive material models followed the guidelines of EN1992-1-2 [17]. The analysis was performed via the software SAFIR2016 [18]. The strength and deformation properties of uniaxially stressed concrete at elevated temperatures are obtained from the stress–strain relationships presented in Figures 2 and 3.

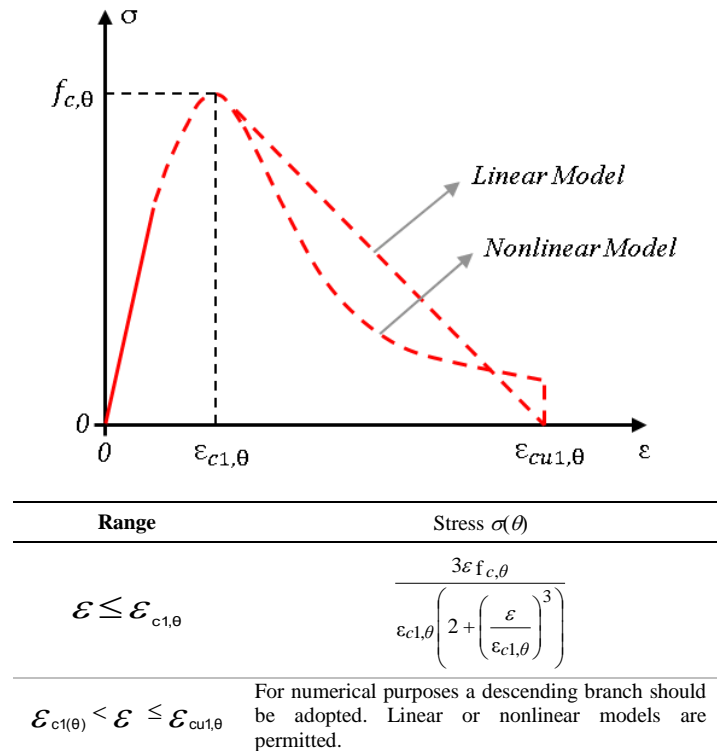


Figure 2. Mathematical model for the stress–strain relationships of concrete under compression at elevated temperatures

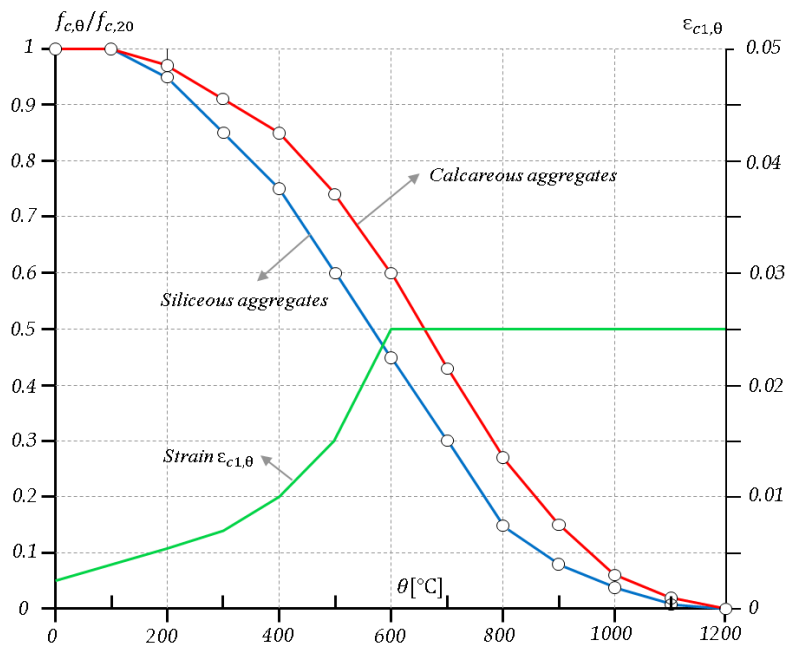
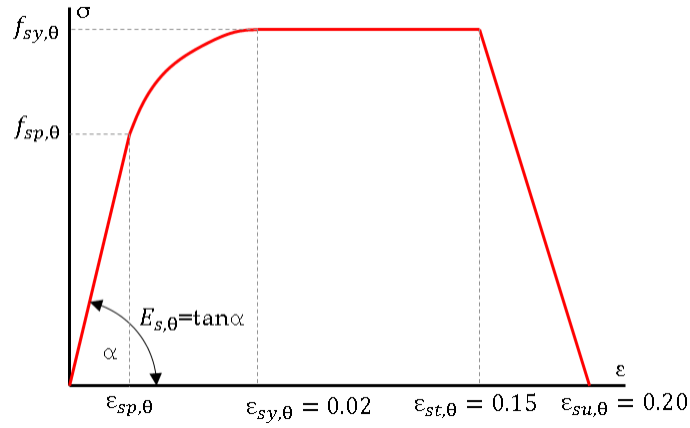


Figure 3. Graphical representation of the main parameters for defining the “stress–dilation” relationships for concretes with siliceous or calcareous aggregates at elevated temperatures

The strength and deformation properties of reinforcing steel at elevated temperatures are obtained from the stress–strain relationships specified in Figures 4 and 5 [17].

The analysis involved creating two separate models with identical geometries: thermal and structural models. The thermal model assessed the transient thermal behavior of the structure under specified thermal loads, incorporating material properties and heat transfer characteristics to evaluate the temperature distributions and thermal gradients throughout the structure. On the other hand, the structural model evaluated the transient mechanical response of the structure subjected to both thermal and mechanical loads. The thermal load data from the thermal model were used to calculate the resulting deformations, stresses, and strains.



Range	Stress $\sigma(\theta)$	Tangent modulus
$\varepsilon_{sp,\theta}$	$\varepsilon E_{s,\theta}$	$E_{s,\theta}$
$\varepsilon_{sp,\theta} \leq \varepsilon \leq \varepsilon_{sy,\theta}$	$f_{sp,\theta} - c + \frac{b}{a} [a^2 - (\varepsilon_{sy,\theta} - \varepsilon)^2]^{0.5}$	$\frac{b(\varepsilon_{sy,\theta} - \varepsilon)}{a [a^2 - (\varepsilon - \varepsilon_{sy,\theta})^2]^{0.5}}$
$\varepsilon_{sy,\theta} \leq \varepsilon \leq \varepsilon_{st,\theta}$	$f_{sy,\theta}$	0
$\varepsilon_{st,\theta} \leq \varepsilon \leq \varepsilon_{su,\theta}$	$f_{sy,\theta} \frac{1 - (\varepsilon - \varepsilon_{st,\theta})}{\varepsilon_{su,\theta} - \varepsilon_{st,\theta}}$	-
$\varepsilon = \varepsilon_{su,\theta}$	0	-
Parameter	$\varepsilon_{sp,\theta} = \frac{f_{sp,\theta}}{E_{s,\theta}}$	$\varepsilon_{sy,\theta} = 0.02; \varepsilon_{st,\theta} = 0.15; \varepsilon_{su,\theta} = 0.20$
Functions	$a^2 = (\varepsilon_{sy,\theta} - \varepsilon_{sp,\theta}) \left(\varepsilon_{sy,\theta} - \varepsilon_{sp,\theta} + \frac{c}{E_{s,\theta}} \right)$ $b^2 = c(\varepsilon_{sy,\theta} - \varepsilon_{sp,\theta})E_{s,\theta} + c^2$ $c = \frac{(f_{sy,\theta} - f_{sp,\theta})^2}{(\varepsilon_{sy,\theta} - \varepsilon_{sp,\theta})E_{s,\theta} - 2(f_{sy,\theta} - f_{sp,\theta})}$	

Figure 4. Mathematical model for the stress–strain relationships of reinforcements steel at elevated temperatures

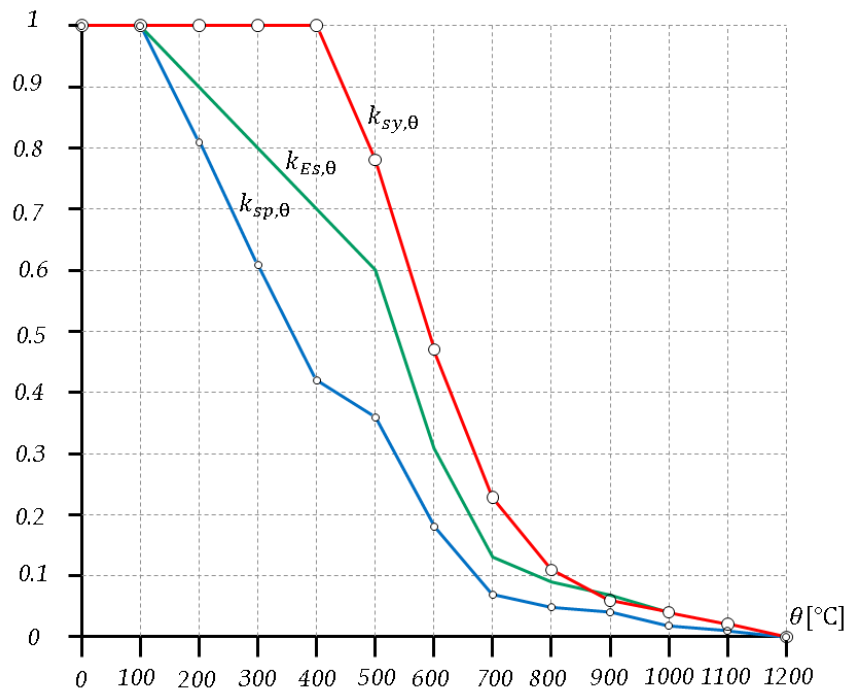


Figure 5. Graphical representation of the reduction coefficients for the parameters of the stress–strain relationship of reinforcing steel at elevated temperatures

The thermal action was defined on the basis of the ISO 834 fire curve (ISO, 1990a), defined by Expression 1 and presented in Figure 6.

$$T_g = 20 + 345 \log(8t + 1) \tag{1}$$

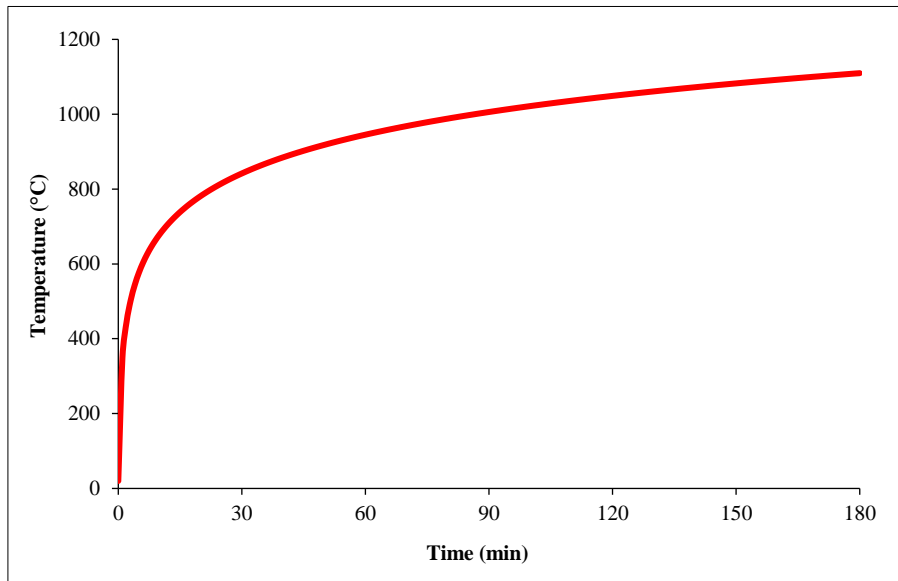


Figure 6. The standard fire ISO 834 curve

3.1. Thermal Analysis

Static analysis of the slabs at each time interval uses the output data from the thermal analysis of the fire-exposed elements, so it should be performed for a compatible finite element mesh, which means performing 2D or 3D thermal analysis, respectively. Considering that in reinforced concrete slabs, the temperature is changed only in the direction of thickness, the cross-section is discretized with rectangular elements with a width equal to the cross-section of the slab. The results for the temperature distribution in the cross section of the slab are equal in the case of 2D or 3D thermal analysis. Figure 7 illustrates the discretization of the slab cross-section with a thickness of 16 cm for the 3D thermal analysis. Figure 8 shows the distribution of the temperature in the cross-section of the slab at $t = 3600$ s (Figure 8a) and $t = 7200$ s (Figure 8b).

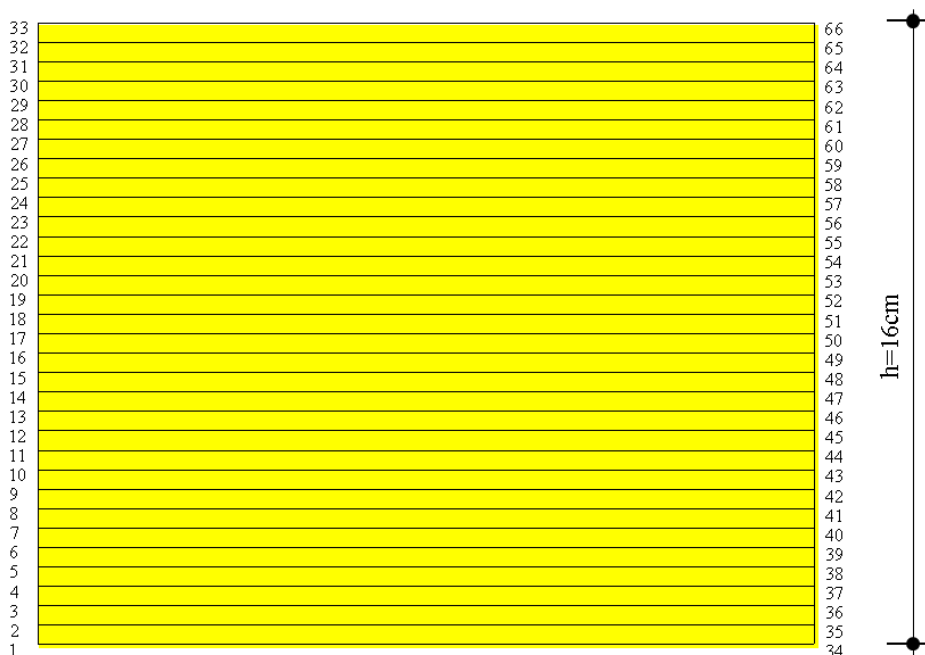


Figure 7. Discretization of the slab cross section via thermal analysis

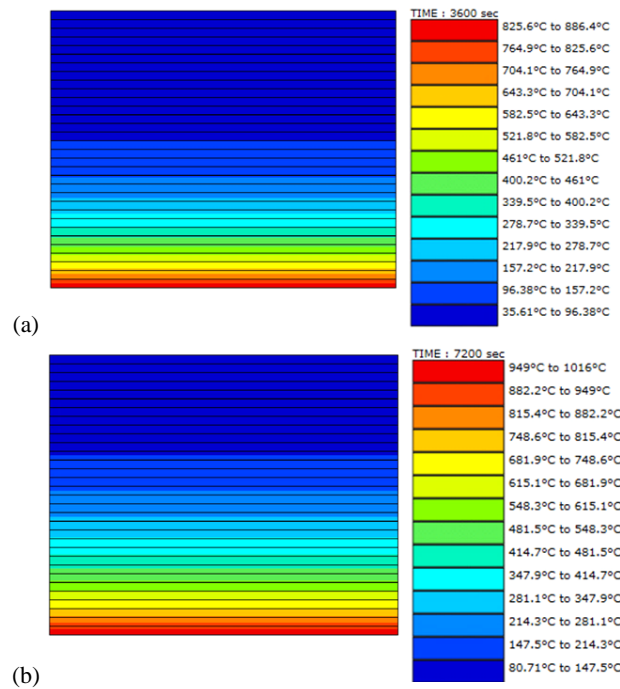


Figure 8. Distribution of the temperature in the slab cross section: a) at time $t = 3600$ s; b) at time $t = 7200$ s

3.2. Structural analysis

A 3D analysis is conducted for the numerical analysis, with discretization performed using shell elements. SAFIR 2016 offers two types of discretization for surface structures in 3D static analysis: one uses a mesh of rectangular shell elements, where the local axes align with the global axes, and the other uses a mesh of quadrilateral shell elements, where the local axes of the shell elements adjust on the basis of the element's geometry. Considering that one-way reinforced slabs exhibit different characteristics in the two orthogonal directions, the x-x axis represents the main direction (and main reinforcement), whereas the y-y axis represents the secondary direction (and secondary reinforcement). Therefore, the discretization of these slabs is performed via rectangular shell elements. The slab is discretized into 256 shell elements, representing its actual width of 5 meters. The boundary conditions and FEM discretization of the slab are shown in Figure 9.

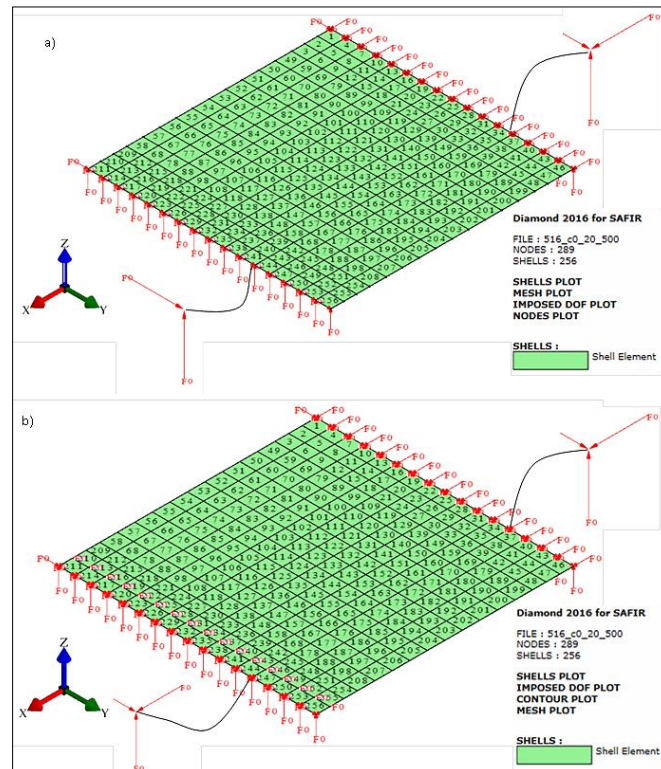


Figure 9. 3D model of a one-way simply supported slab with boundary conditions and discretization: a) axially unrestrained; b) fully axially restrained

4. Validation

4.1. Validation of the SAFIR2016 Software for Thermal Analysis

Figure 10 presents a comparison of temperatures in a 150 mm thick slab subjected to the standard ISO 834 fire exposure obtained by SAFIR2016 and experimental tests in the PCA (Portland Cement Association) laboratory [19, 20]. The diagrams show that in the first 60 minutes, the SAFIR2016 program gives approximate temperatures of the experimental results. After 120 minutes, the difference in the results was more significant. To ensure a match of the experimental and numerical results, it is necessary to define all the material properties of the concrete and steel accurately. In the example, they are assumed, that is, they are adopted according to the recommendations given in EN 1992-1-2 [17].

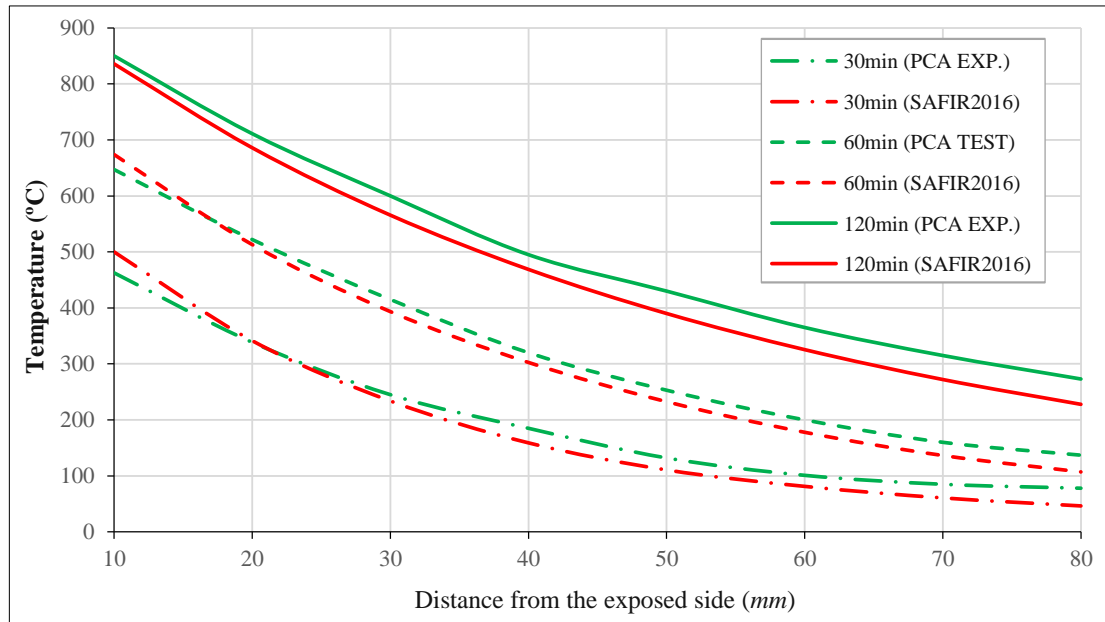


Figure 10. Comparison of temperatures in a 150 mm thick slab obtained with SAFIR2016 and experimentally obtained data given by Terro et al. [20]

4.2. Validation of the Software SAFIR2016 for Structural Analysis

To verify the SAFIR2016 program for one-way simply supported slabs, the results of the experimental research conducted at the WFR (Warrington Fire Research Center) organized by the BRE (Building Research Establishment) will be used [21]. One-way simply supported slabs, with span $L=4.5$ m, width $b=0.93$ m and thickness $h=0.15$ m, were tested. The slabs in the longitudinal direction are reinforced with 10 bars with a diameter of 8 mm at a distance of 90 mm, and in the transverse direction, the bars have a diameter of 8 mm and are spaced 600 mm apart. The concrete cover is 25 mm long. One of the slabs is tested with a load of 1.5 kN/m², whereas the other slab is unloaded. The compressive strength of the concrete after 28 days is 52 MPa. More detailed data about the experiment are given in the literatures [22-24].

Typically, one-way load-bearing slabs are analyzed as 1-m-wide strips, i.e., 1-m-wide beam elements, whereas two-way load-bearing slabs are analyzed with shell elements. The question arises as to whether this approximation of slabs bearing in one direction is also suitable for slabs exposed to fire action. For this reason, the slabs analyzed with the SAFIR2016 program are discretized with both 2D beam elements and 3D shell elements, and the results are compared with the experimentally obtained values.

Figures 11 and 12 show the experimentally obtained vertical displacements of the slab [21], which are compared with the displacements obtained by SAFIR2016. The shapes of the curves of the vertical plate displacements over time for both the 2D and 3D analyses are identical, but owing to the greater stiffness of the beam element relative to the stiffness of the shell element, the displacements are greater.

The advantage of 3D analysis is that the shell element includes membrane forces, but in the concrete tested slabs, the real width is less than 1 m, the membrane forces in the transverse direction are weakly expressed, and the slab behaves more like a freely supported beam. Therefore, the results obtained from the 2D analysis are closer to those of the experimental results.

In the general case, for slabs with real widths, 3D analysis is expected to yield more realistic results, but for practical reasons (shorter calculation time), 2D analysis can also be applied, the results of which have satisfactory accuracy.

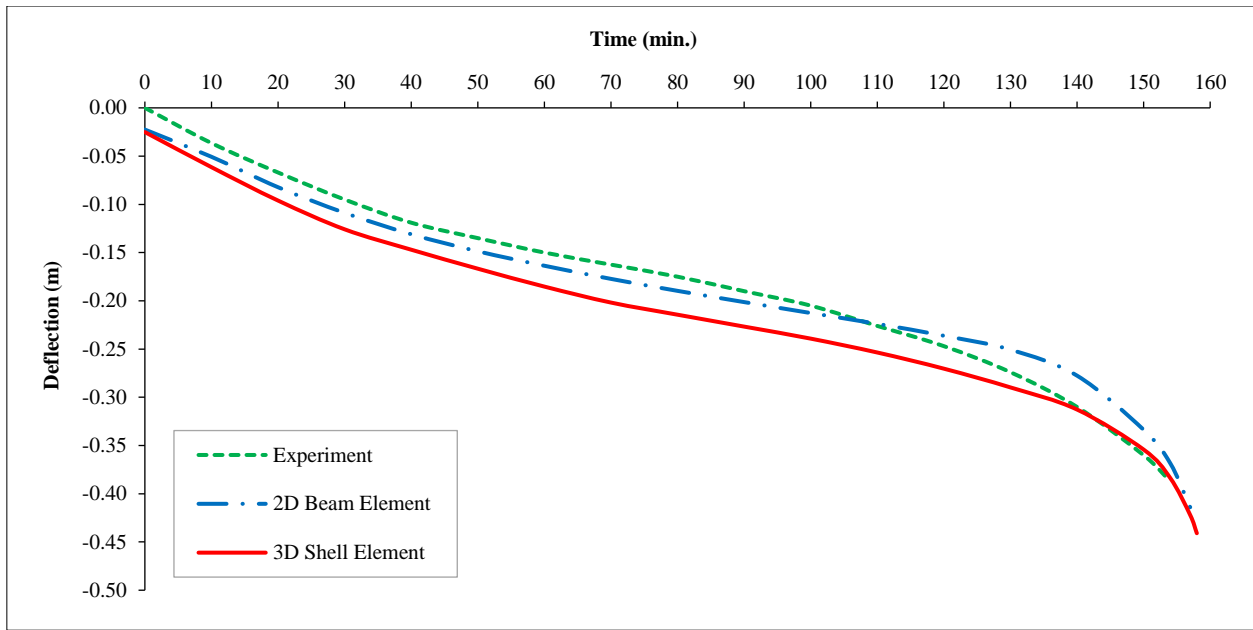


Figure 11. Comparison of experimentally measured displacements of a loaded slab [21] with numerically calculated values with SAFIR2016

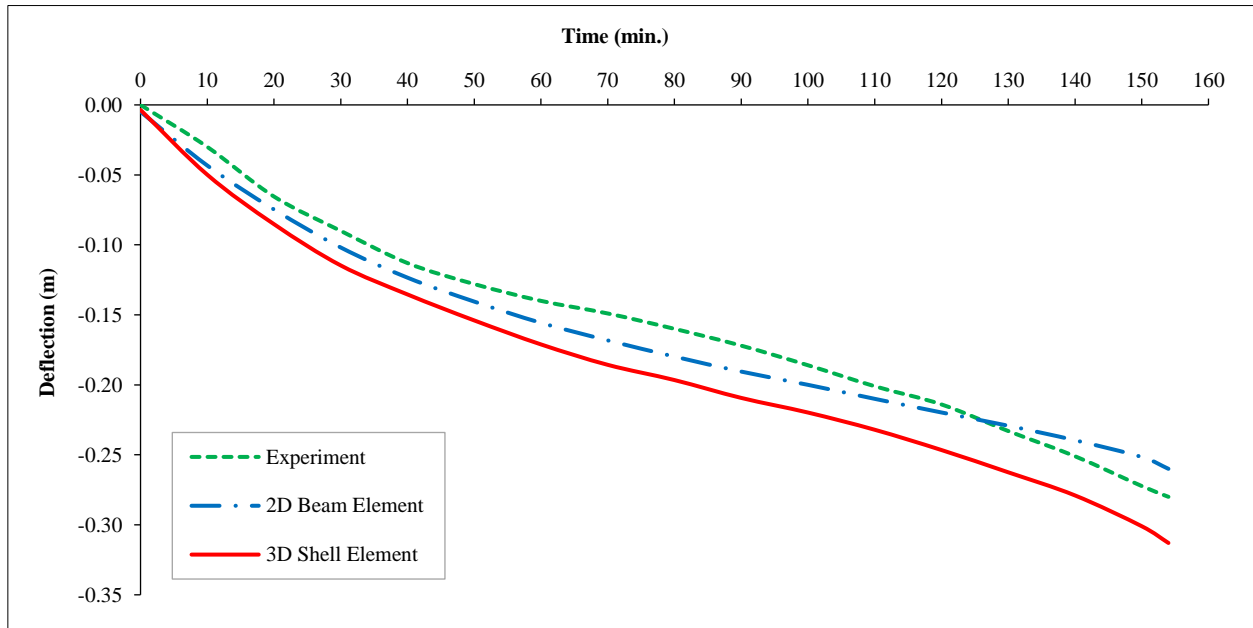


Figure 12. Comparison of experimentally measured displacements of the unloaded slab [21] with numerically calculated values with SAFIR2016

5. Results and Discussion

5.1. Slabs Exposed to Fire from the Bottom

The analysis aims to define the effects of the axial restraint and the fire scenario. In Figure 13, the RC slab that was analyzed is described. The design actions for fire situations are defined according to the recommendations given in EN 1992-1-2 [17].

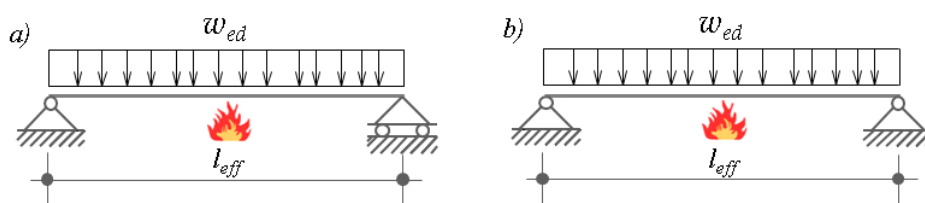


Figure 13. Static scheme of the slab: a) axially unrestrained; b) fully axially restrained

The common properties of the analyzed slabs are shown in Table 1.

Table 1. Slab properties

Slab thickness, h	16 cm
Concrete compressive strength, f_{ck}	30 MPa
Concrete model	EN 1992-1-2
Concrete aggregates	Siliceous
Reinforcing steel yield strength, f_{yk}	500 MPa
Steel model (thermal and mechanical)	Hot rolled (EN 1992-1-2)
Dead load (including self-weight), g_k	5.5 kN/m ²
Live load, q_k	4.0 kN/m ²
The design load for ambient temperature, E_d	13.425 kN/m ²
Fire load, $E_{d,fi}$ [17]	7.9 kN/m ²

The adopted main reinforcement area with a concrete cover thickness of 2.0 cm for different slab spans is presented in Table 2.

Table 2. Adopted main reinforcement area for different slab spans

Slab span, L (m)	Adopted main reinforcement $A_{s1,x}$ (cm ² /m)
4.0	4.831
5.0	7.778
6.0	11.668

5.1.1. One-Way Simply Supported Reinforced Concrete Slabs without Axial Restraint

Salihu et al. [25] investigated the fire resistance of one-way simply supported reinforced concrete slabs without axial restraint through 3-dimensional numerical analyses via SAFIR2016 software. Their parametric studies focused on evaluating the impact of the concrete cover thickness and span length. Figure 14 displays the vertical displacements of slabs with span lengths of $L = 4$ m, $L = 5$ m, and $L = 6$ m under fire exposure. The figure shows that the fire resistance of the analyzed slabs is 114 minutes.

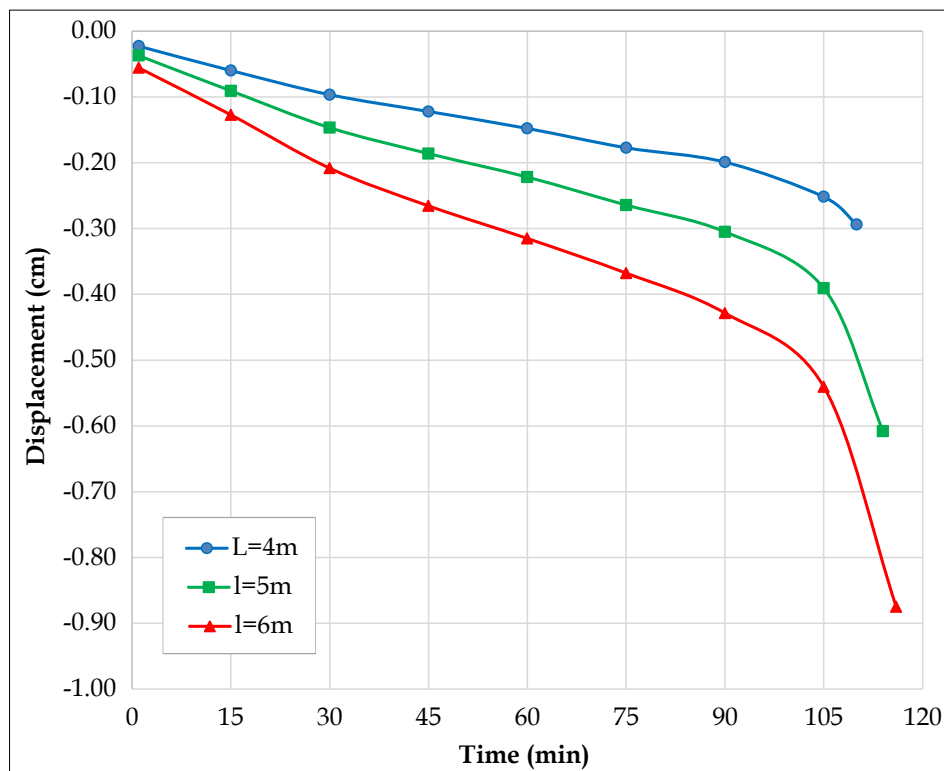


Figure 14. Vertical displacement in the midspan of one-way simply supported slabs axially unrestrained

• **Bending Moments and Axial Forces in One-Way Simply Supported Slabs without Axial Restraint**

Owing to the slab's symmetry, the analysis focuses solely on the axial forces and bending moments for one-half of the slab. Figure 15 shows the bending moments in the longitudinal direction, revealing a notable difference in the diagrams of these moments. After 90 minutes, the bending moments remained relatively constant. The support conditions of the slab did not significantly influence the bending moment distribution near the supports. However, a larger variation in the distribution of bending moments is evident in the midspan of the slab.

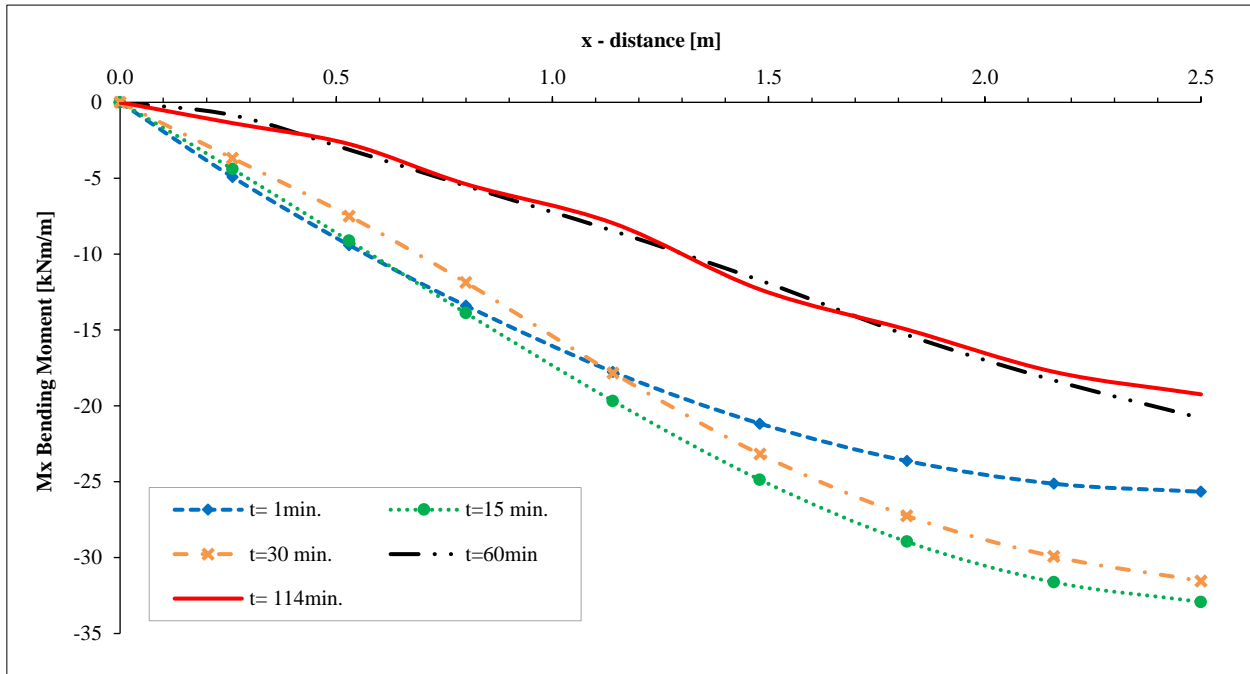


Figure 15. Bending moments (kNm/m) in the longitudinal direction on one-way simply supported slabs axially unrestrained

On the basis of the equilibrium of horizontal forces in both the X- and Y-directions, any cross-section of Pin-Pin-supported slab without restraints in these directions must have a total membrane force of zero.

As illustrated in Figure 16, the membrane forces in one-way slabs under fire exposure act as self-balancing horizontal forces. In contrast, the membrane forces in these slabs under ambient conditions are zero.

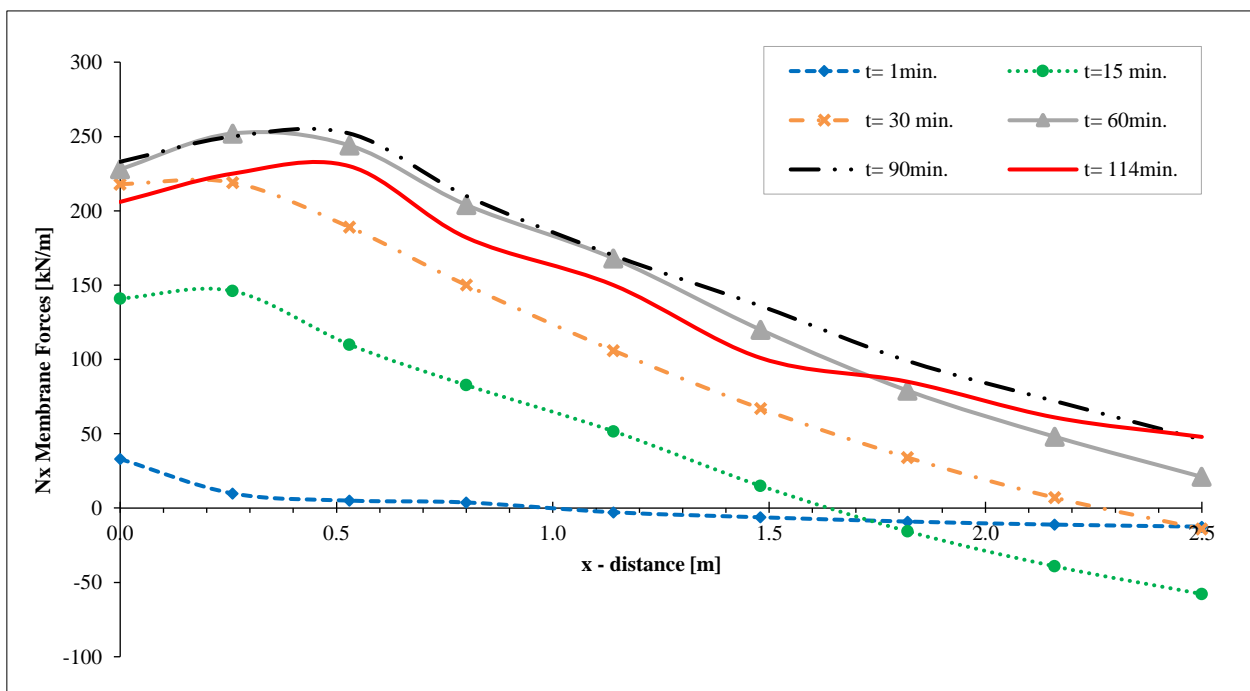


Figure 16. Membrane forces (kN/m) in the longitudinal direction on one-way simply supported slabs axially unrestrained

• **Concrete and Reinforcement Stresses in One-Way Simply Supported Slabs without Axial Restraint**

Figure 17 shows the concrete compressive stresses over time on the section at the midspan, obtained via SAFIR2016 software. Both vertical loads and fire exposure from the underside cause compressive stresses in the upper fibers. The vertical loads induce bending in the slab, resulting in compressive stresses in the upper fibers. Moreover, fire induces nonlinear temperature variations and thermal expansion changes, which generate thermal stresses in the slab.

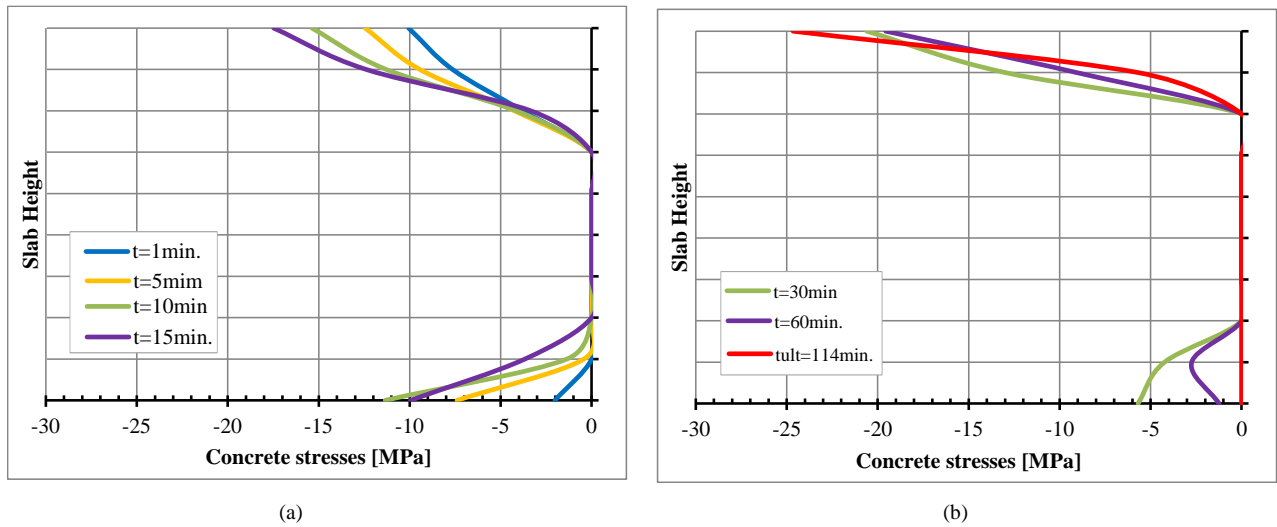


Figure 17. Evolution of concrete stresses over time in the slab cross-section at midspan: a) During the first 15 minutes; b) From 30 minutes until failure

The fulfillment of Bernoulli's hypothesis is a prerequisite for slabs with a high span-to-depth ratio, suggesting that plane cross sections must remain planar. This forms compressive stresses in the bottom fibers from mechanical dilatations (Figure 17). The stresses due to temperature changes are most significant during the first 30 minutes of the fire when the stiffness of the element is relatively high.

Figure 18 shows the tensile reinforcement stresses over time on the section at the midspan, as obtained via numerical analysis. For the lower reinforcement that is heated, an apparent stress reduction occurs due to the decrease in the tensile strength of the steel. When the values are expressed as a percentage of the steel's current load capacity, it becomes evident that they are close to the steel's yield strength, as shown in Figure 19.

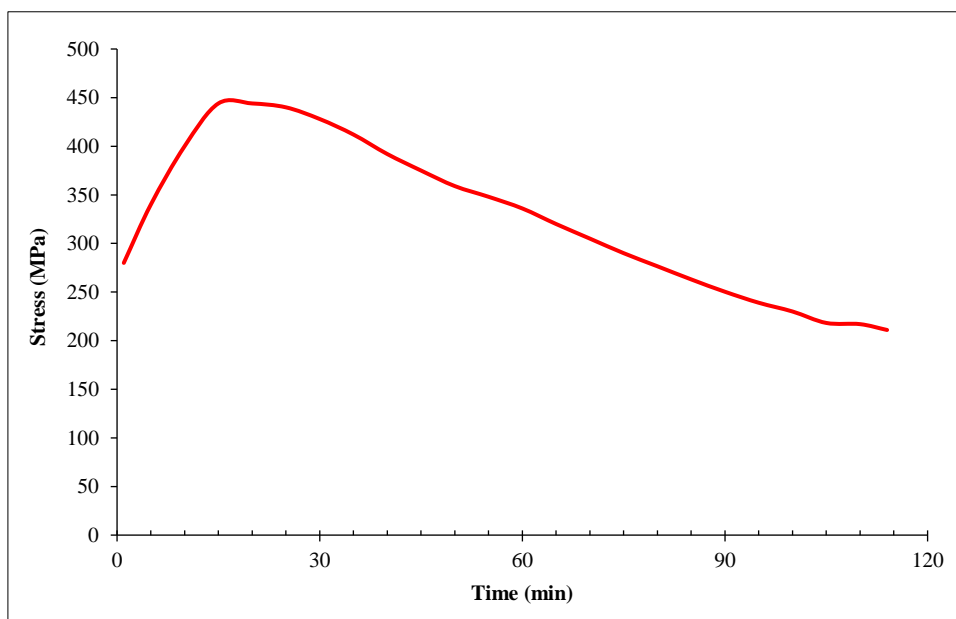


Figure 18. Stresses in the main reinforcement over time at the midspan cross section

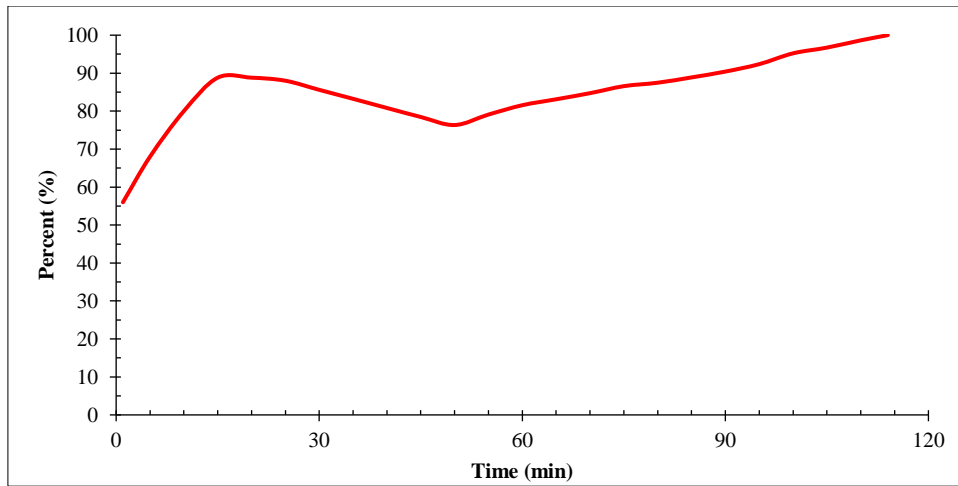


Figure 19. Stresses in the main reinforcement over time at midspan, expressed as a percentage of the current yield strength of the steel

5.1.2. One-Way Simply Supported Reinforced Concrete Slabs with Axial Restraint

• Bending Moments and Axial Forces in One-Way Simply Supported Slabs with Axial Restraint

From the perspective of the initiated bending moments, during the first 15 minutes, as the negative axial force increases, the horizontal reaction at the support points contributes to the rise in the bending moment in the span caused by the external loads. This effect is expressed in relation to the reference axis for the section in its deformed state, where the center of the section is lower than the support point. At $t = 15$ minutes, the bending moment reaches its maximum value. Once the axial force reaches zero, the bending moment returns to its initial value (point 2 in Figure 22) and then changes direction. The reversal in sign occurs due to the reaction at the support, which, as the membrane tension forces increase (Figure 21), changes direction and generates a reverse moment counteracting the moment caused by the external loads (Figure 20).

Figure 22 shows the time variation of the bending moment at the midspan of a simply supported slab with a span of $L = 5$ m subjected to restrained axial expansion during fire exposure from the bottom. The negative sign indicates a moment that results in tension in the lower part of the slab. As shown in the diagram, for the slab with restrained axial expansion, the bending moment increases rapidly during the initial phase of the fire, reaching its peak at the 15th minute (point 1 in Figure 22), after which it begins to decrease. This behavior occurs because, in the early stages, only a tiny portion of the heated lower zone experiences extremely high temperatures, whereas the rest of the cross-section remains cool. This leads to the development of considerable compressive stresses in the heated fibers and tensile stresses in the cooler fibers of the cross-section.

The total axial force is negative and gradually increases during the first 15 minutes (point 1 in Figure 23). As the fire progresses and the temperature spreads deeper into the slab, the axial force decreases and eventually reaches zero (point 2 in Figure 23). After approximately 30 min, the temperature variations across the cross-section become more uniform, resulting in increased slab displacement and the onset of membrane tension forces, which progressively intensify. The timing of the peak bending moment and its subsequent decrease depend on the thickness of the slab.

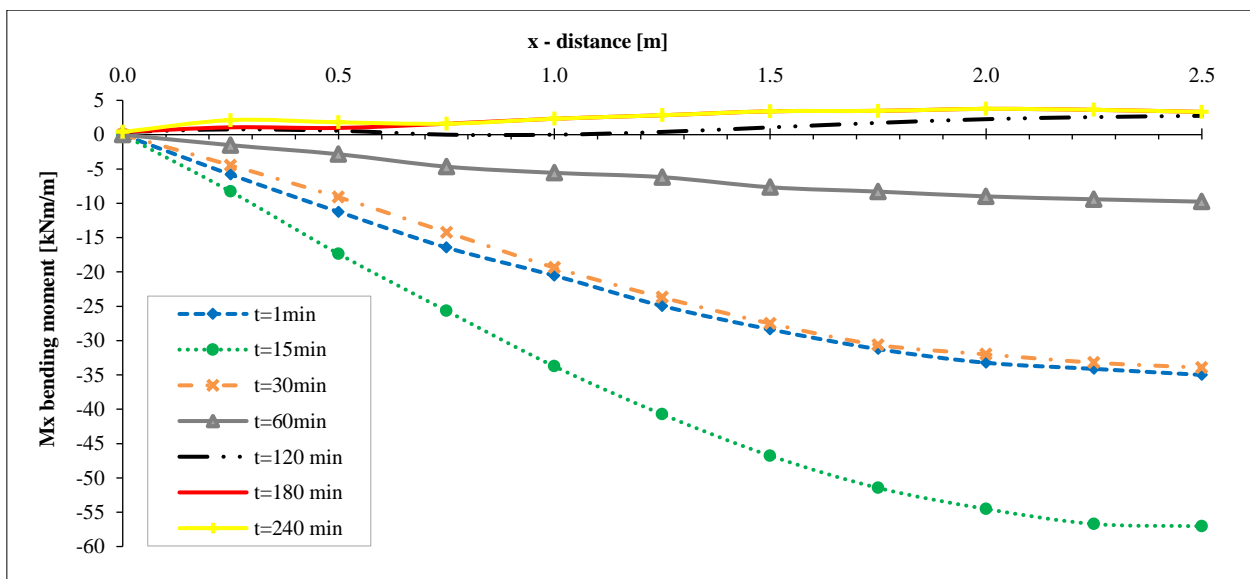


Figure 20. Bending moments (kNm/m) in the longitudinal direction on one-way simply supported slabs axially restrained

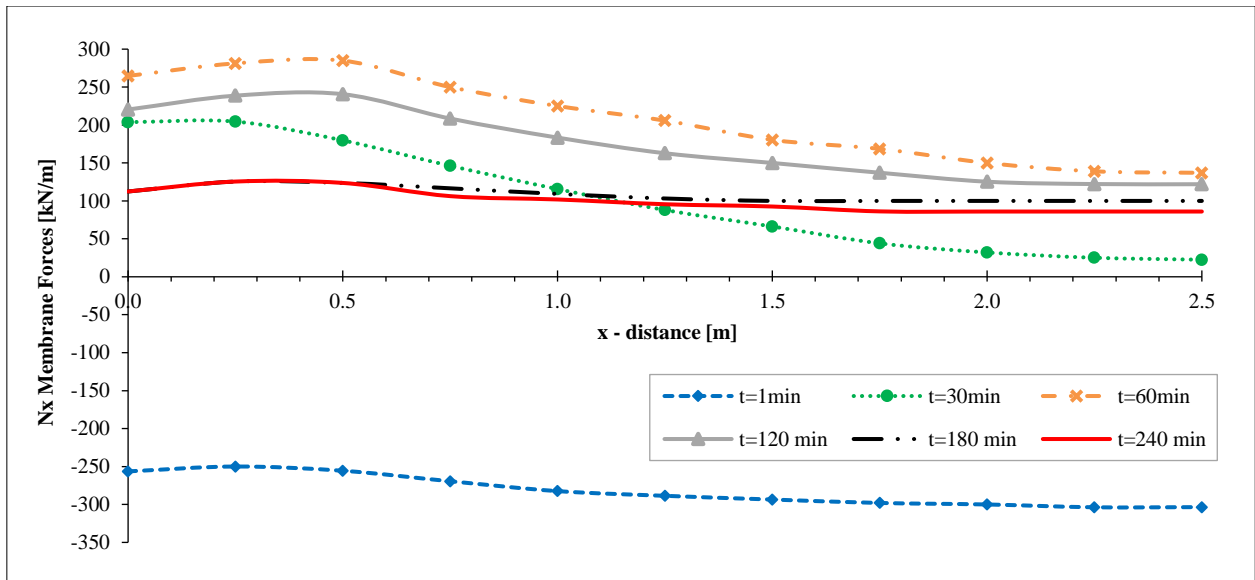


Figure 21. Membrane forces (kN/m) in the longitudinal direction on one-way simply supported slabs axially restrained

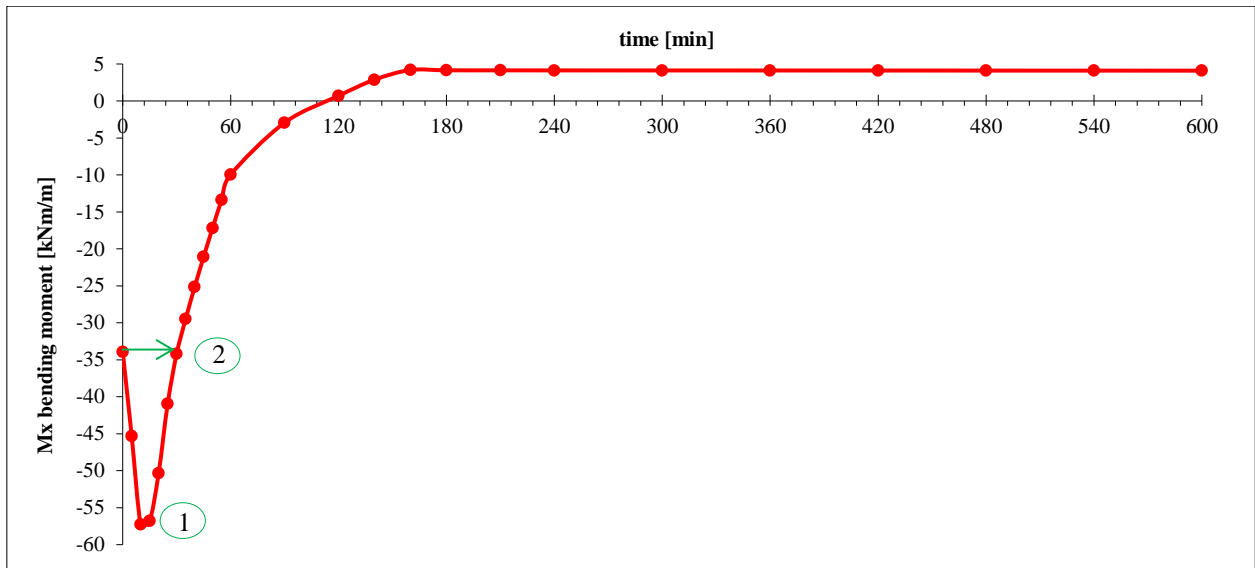


Figure 22. Time evolution of the bending moment (kNm/m) in span for a simply supported slab with a span $L=5$ m, obtained via 3D analysis

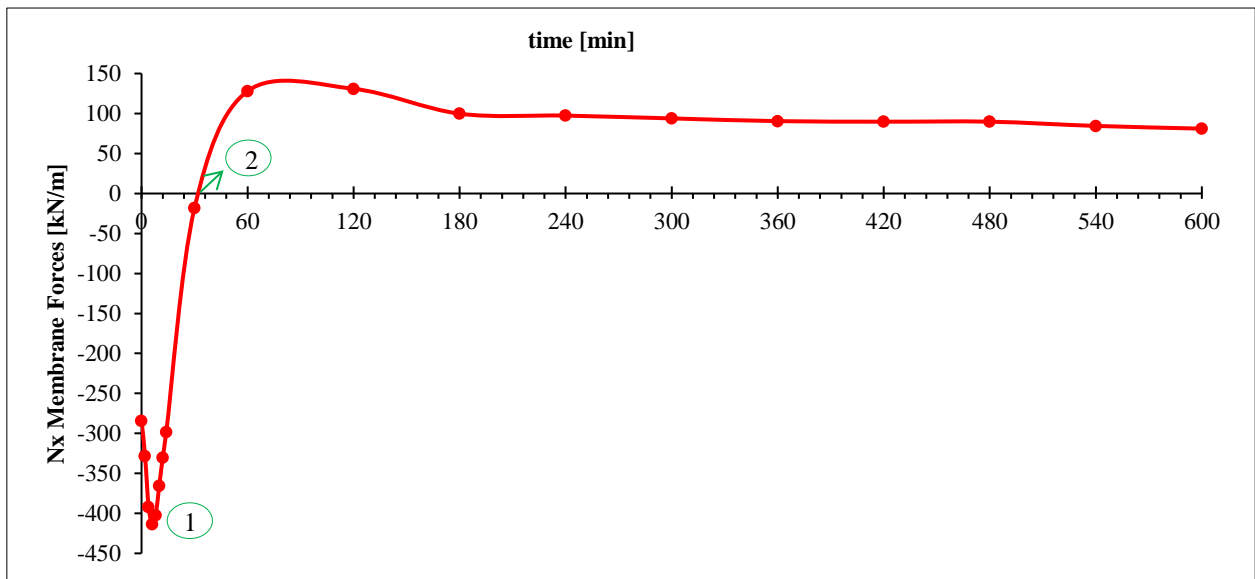


Figure 23. Time evolution of the axial force (kN/m) in span for a simply supported slab with a span $L=5$ m axial restraint, obtained via 3D analysis

For larger spans ($l = 6\text{ m}$), the initial vertical displacements caused by the loads are more significant, causing the membrane tension forces to become more prominent earlier. These forces eventually surpass the compressive forces generated by temperature differences, resulting in a smaller peak in the moment diagram (point 1 in Figure 24).

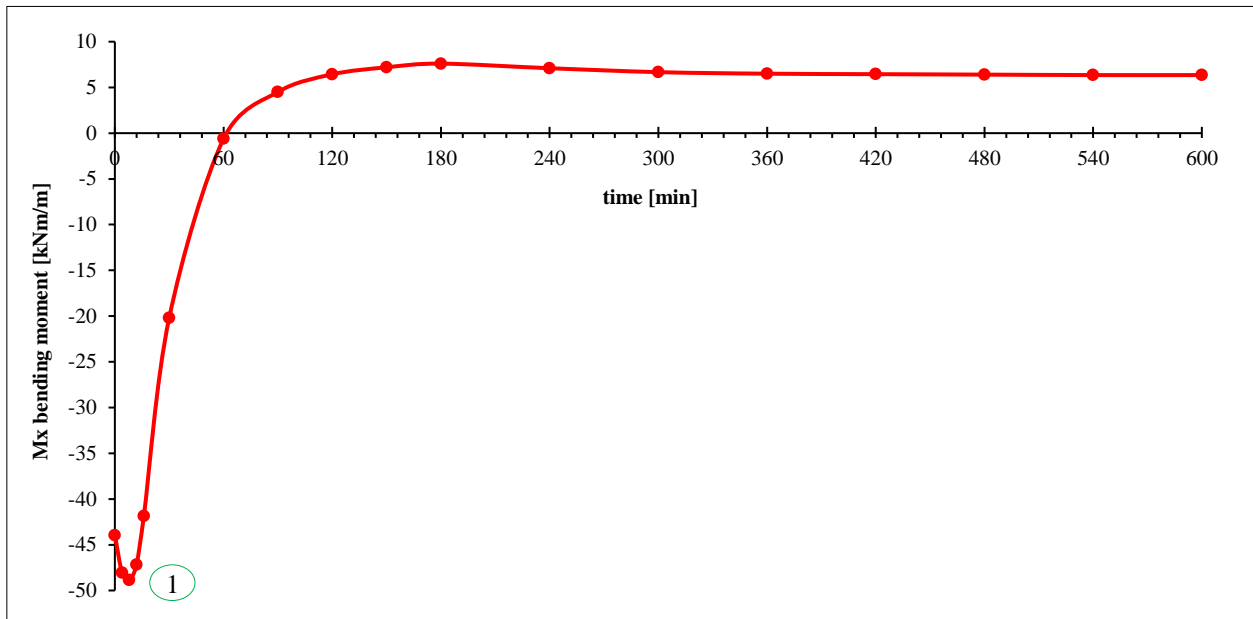


Figure 24. The time evolution of the bending moment in the span of a simply supported slab with a span of $l = 6\text{ m}$, subjected to prevented axial dilation, as obtained through 3D analysis.

• **Concrete and Reinforcement Stresses in One-Way Simply Supported Slabs with Axial Restraints**

Figure 25 shows the concrete compressive stresses over time up to 6 hours on the section at the midspan, which were obtained via SAFIR2016 software. Both vertical loads and fire exposure from the underside cause compressive stresses in the upper fibers. The vertical loads induce bending in the slab, resulting in compressive stresses in the upper fibers. Moreover, fire induces nonlinear temperature variations and thermal expansion changes, which generate thermal stresses in the slab.

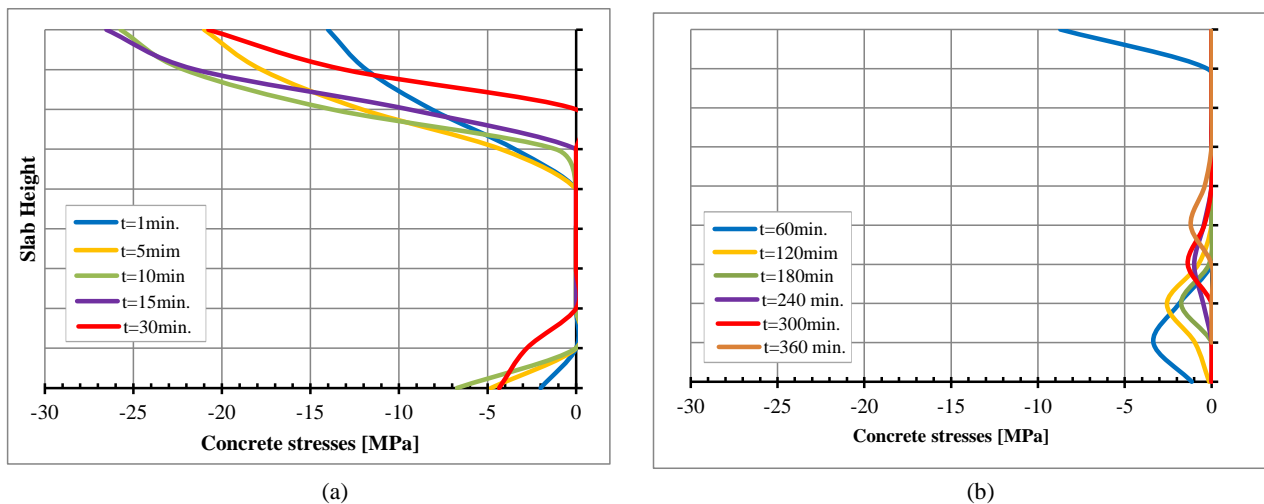


Figure 25. Evolution of concrete stresses over time in the slab cross-section at midspan: a) In the first 30 minutes; b) From the first hour to the sixth hour

After 1 hour of fire action, on the basis of the axial force diagram (Figure 23), the slabs begin to work in tension, where the tensile force is accepted by the pinned supports, the external load is resisted only by the reinforcement, and the stresses in the concrete are almost zero (Figure 25b).

Figure 26 shows the stresses in the lower and upper reinforcements of a slab with a span of $l = 5\text{ m}$, where axial expansion is prevented. As the bending moment increases in the field, the stresses in both the lower tension reinforcement and the upper compression reinforcement also increase (point 1 in Figure 26). Following this, as the bending moment decreases, there is a slight reduction in the stresses of the tension reinforcement. However, with increasing vertical displacement, the membrane tensile forces intensify, causing the tensile stresses in both the lower

and upper reinforcement zones to rise. In the diagram in Figure 23, the stresses in the lower reinforcement appear to decrease because they are presented in MPa rather than as a percentage of the steel's instantaneous bearing capacity at the corresponding temperature.

The lower reinforcement yields after 3 hours (or 10,800 s) of fire exposure (Figure 26). Moreover, the upper reinforcement at the midspan reaches the yield strength of the steel at the appropriate temperature after 2.5 hours of exposure (point 3 in Figure 26). At this point, a plastic hinge forms, and the slab transitions into a catenary, with the load-bearing capacity being provided by membrane tension forces in both directions. For the slab to effectively absorb these tensile forces, reinforcement in the upper zone within the span is essential.

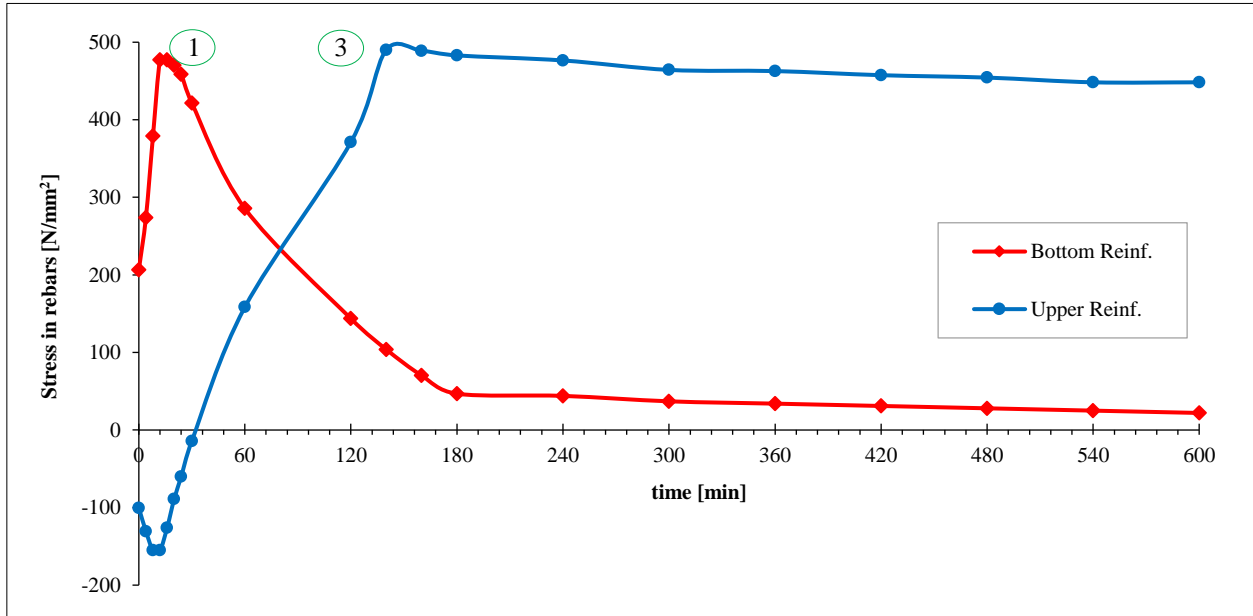


Figure 26. Time evolution of the stresses in the reinforcement in a span in a simply supported slab with a span $L=5$ m, with axial restraint, 3D analysis

The induced stresses in the reinforcing bars are shown in Figure 27. In this case, the reinforcement in the lower zone yields after 3 hours (point 2 in Figure 27). The dashed line illustrates the reduction in the steel yield strength due to the temperature of the reinforcement. When the stresses in the reinforcement reach the yield strength, the reinforcement yields, and a plastic hinge forms, causing the slab to behave as a catenary. The stresses in the upper zone reinforcement approach the yield strength earlier (point 1 in Figure 27) because it remains in the cooler zone, where the temperature does not induce additional compressive stresses or relieve them, as is the case with the lower reinforcement.

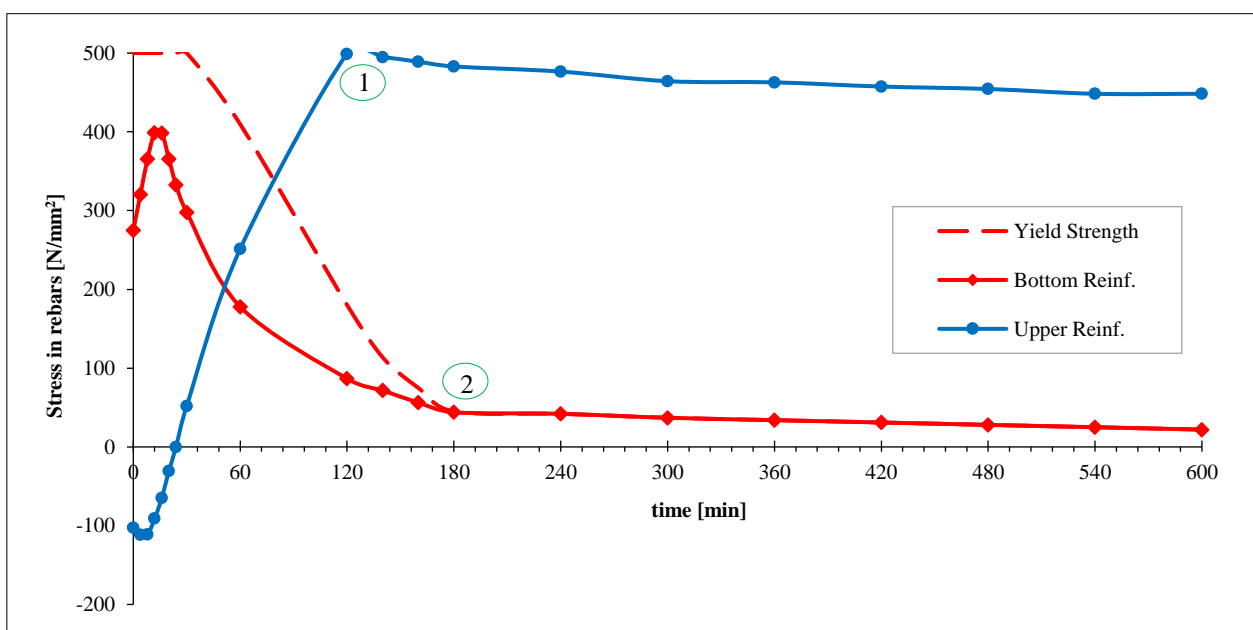


Figure 27. The time-dependent evolution of stresses in the reinforcement within the span of a supported slab with a span of $L = 6$ m, subjected to prevented axial dilatation, as analyzed through a 3D approach

5.1.3. Comparison of the Fire Resistance Between One-Way Simply Supported Slabs without Axial Restraint and Those With Full Axial Restraint Exposed to Fire from the Bottom

Figure 28 shows the vertical displacement of the slabs obtained via 3D analysis. A comparison of the vertical displacement of the slabs when they are axially unrestrained and axially restrained is shown. Evidently, preventing axial restraint significantly increases the fire resistance of one-way simply supported reinforced concrete slabs and reduces vertical displacement.

From the aspect of the criteria of allowed displacements, the axial restraint slabs reach the displacement limit value, which, in the case of fire, is $L/30$ for a period of 10 minutes earlier than the axial unrestraint slabs. In the first few minutes, due to axial restraint, the vertical displacements are greater, but then, the membrane tensile forces are activated, which contributes to the reduction in vertical displacement and, at the same time, increases the fire resistance of the slabs.

In addition to higher fire resistance, the time–displacement curves for axially restrained slabs differ from those for axially unconstrained slabs. In axially unconstrained slabs, the asymptote of the time–displacement curves at failure is vertical, whereas in axially restrained slabs, the asymptote of the time–displacement curves tends to become horizontal (Figure 28).

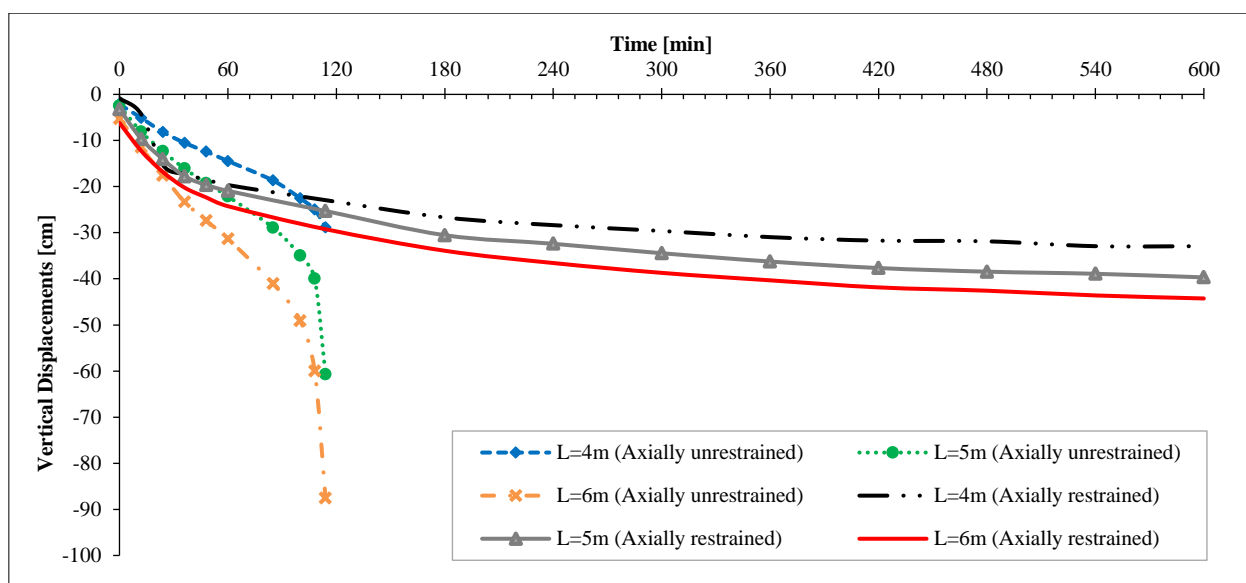


Figure 28. Comparison of the vertical displacements in the midspan of the axially restrained and axially unrestrained slabs obtained via 3D analysis

Table 3 presents the results of the analysis conducted for the fire resistance of one-way simply supported reinforced concrete slabs axially restrained and axially unrestrained for various spans. The results indicate that axial restraint increases the fire resistance of one-way, simply supported reinforced concrete slabs. According to the load-bearing criteria, all the analyzed axial restraint slabs exhibited fire resistance greater than 10 hours. A ten-hour numerical analysis was conducted to observe the behavior of the slabs over time, with the goal of clearly identifying the parameters that define their resistance. Regarding the criterion for allowable displacements $L/30$, it should be noted that the slenderness ratio of the slabs L/h has a certain effect. Slabs with a higher slenderness ratio reach an earlier allowable displacement of $L/30$.

Table 3. The impact of the slab span and axial restraint on the fire resistance of slabs exposed to fire from the bottom side, according to failure criteria and allowable deflection criteria

Slab span, L (m)	Fire resistance (minutes)			
	Axially unrestrained slabs		Axially restrained slabs	
	Failure	Deflection $L/30$	Failure	Deflection $L/30$
4	114	43	>600	15
5	114	32	>600	31
6	116	26	>600	35

5.2. Slabs Exposed to Fire from the Top Side

In practice, there are two possible scenarios for slabs exposed to fire: the fire can act from the bottom or from the top (Figure 29). The scenario of fire acting from both sides has not been considered, as Eurocode guidelines [1] recommend that fire exposure is limited to a single fire sector.

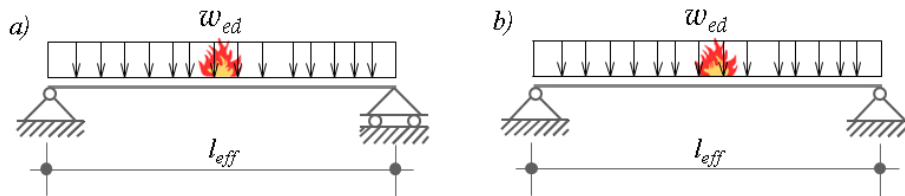


Figure 29. Simply supported slab exposed to fire from the top: a) axially unrestrained; b) axially restrained

5.2.1. One-Way Simply Supported Reinforced Concrete Slabs without Axial Restraint

When fire acts from the top of simply supported one-way slabs with axial unrestraint, their fire resistance exceeds 10 hours (Figure 30). Figure 30 displays the vertical displacements at the midspan of the slab for static spans of $L = 4$ m, $L = 5$ m, and $L = 6$ m. The fire effect causes the slabs to deflect upward.

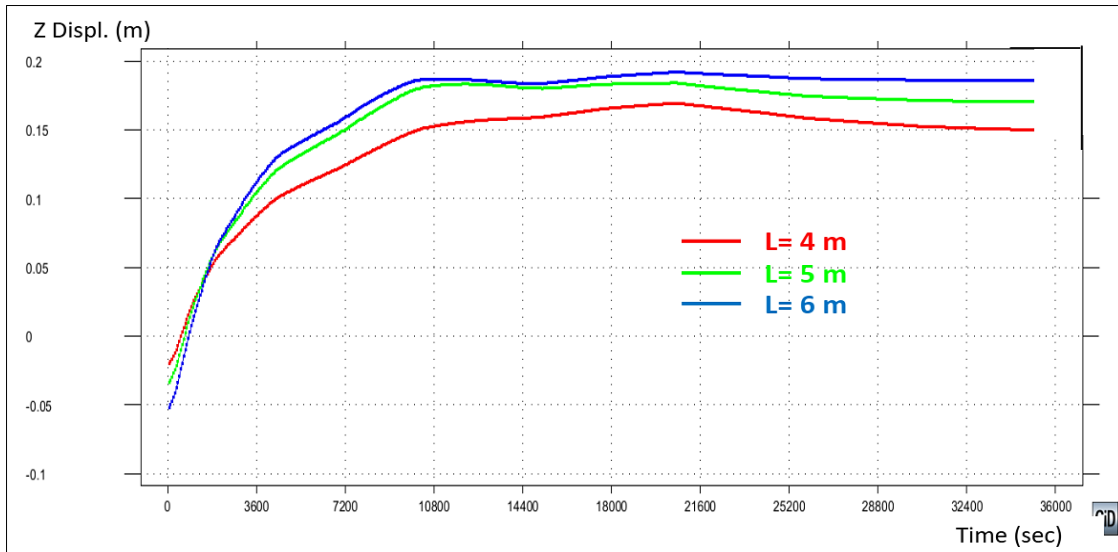


Figure 30. Vertical displacements in the span of axially unrestrained slabs with spans $L=4$ m, $L=5$ m and $L=6$ m exposed to fire from the top

• Bending Moments and Axial Forces in One-Way Simply Supported Slabs without Axial Restraint

Figure 31 shows the bending moments in the longitudinal direction, revealing a notable difference in the diagrams of these moments. The bending moment envelope is observed during the first 30 minutes of fire exposure. Starting from a maximum moment of 25.40 kNm at the midspan, the moment decreases to 15.80 kNm after 30 minutes. This reduction is due to the increased stiffness of the slab. As the temperature increases through the depth of the slab, the modulus of elasticity of the material decreases, causing the bending moments to stabilize at nearly constant values after the second hour of fire exposure.

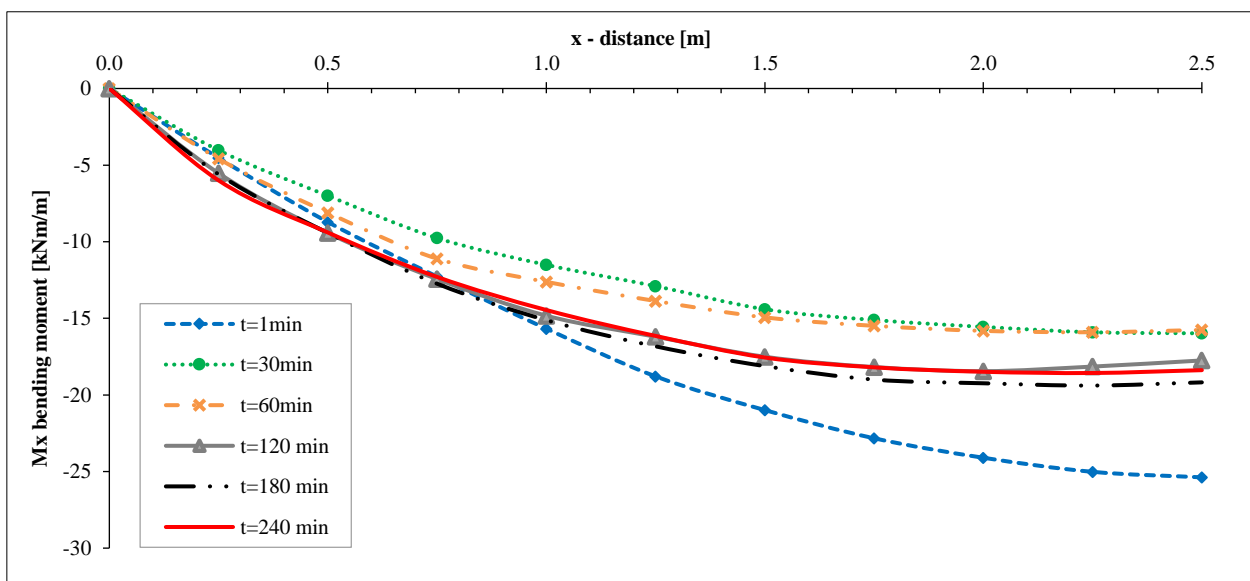


Figure 31. Bending moments (kNm/m) in the longitudinal direction on one-way simply supported slabs axially unrestrained

On the basis of the equilibrium of horizontal forces in both the X- and Y-directions, any cross-section of Pin-Pin-supported slab without restraints in these directions must have a total membrane force of zero. As illustrated in Figure 32, the membrane forces in one-way slabs under fire exposure act as self-balancing horizontal forces. In contrast, the membrane forces in these slabs under ambient conditions are zero.

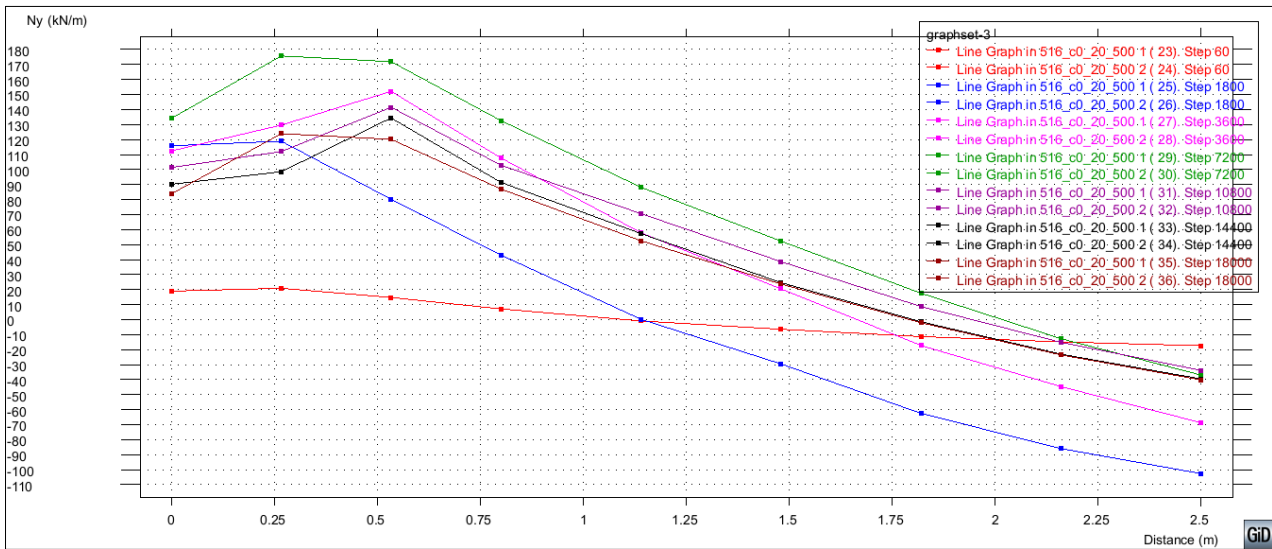


Figure 32. Membrane forces (kN/m) in the longitudinal direction on one-way simply supported slabs axially unrestrained

• Concrete and Reinforcement Stresses in One-Way Simply Supported Slabs without Axial Restraint

Figure 33 shows the concrete compressive stresses over time up to 6 hours on the section at the midspan, which were obtained via SAFIR2016 software. The vertical loads induce bending in the slab, resulting in compressive stresses in the upper fibers exposed to fire, whereas fire exposure from the top side causes compressive stresses in the lower fibers, which are at ambient temperature. Owing to the opposing action of external loads and thermal stresses, as well as the possibility of free axial expansion of the slab, in this case, the slab has high fire resistance.

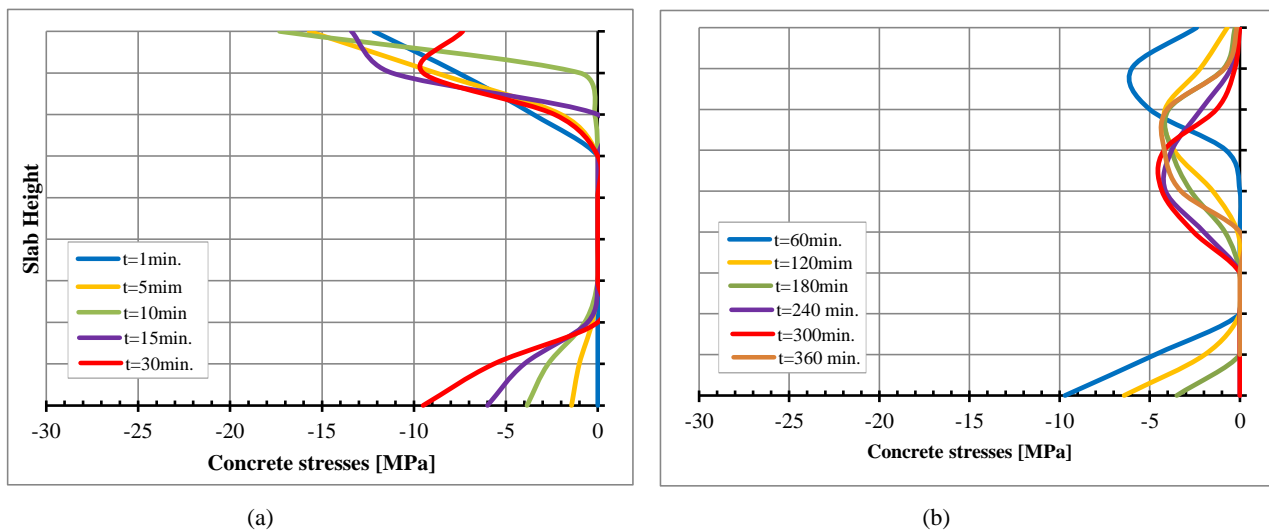


Figure 33. Evolution of concrete stresses over time in the slab cross-section at midspan: a) In the first 30 minutes; b) From the first hour to the sixth hour

When the fire acts from above, the main reinforcement is positioned in the lower zone, where the maximum temperature during the entire 10-hour exposure reaches 340°C. At these temperatures, the tensile strength of the reinforcement remains unaffected. As a result, the slabs exhibit high fire resistance, with no failure occurring even after 10 hours of exposure (Figure 34).

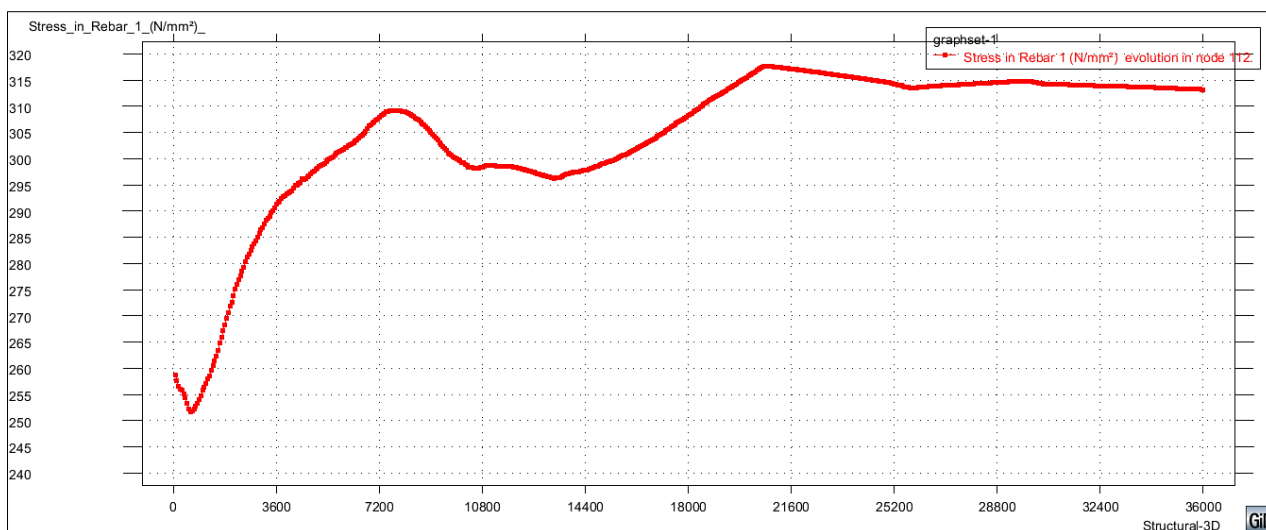


Figure 34. Time evolution of the stresses in the reinforcement at the midspan in a simply supported slab with a span of L=5 m, with axial unrestraint, 3D analysis

5.2.2. One-Way Simply Supported Reinforced Concrete Slabs with Axial Restraint

Figure 35 shows the vertical displacements of a slab with a static span of L=5 m, which is axially restrained and exposed to fire from above. The fire effect causes the slab to move upward, and at the point of failure, occurring at 339 minutes, the slab has risen by 30 cm at the mid-span.

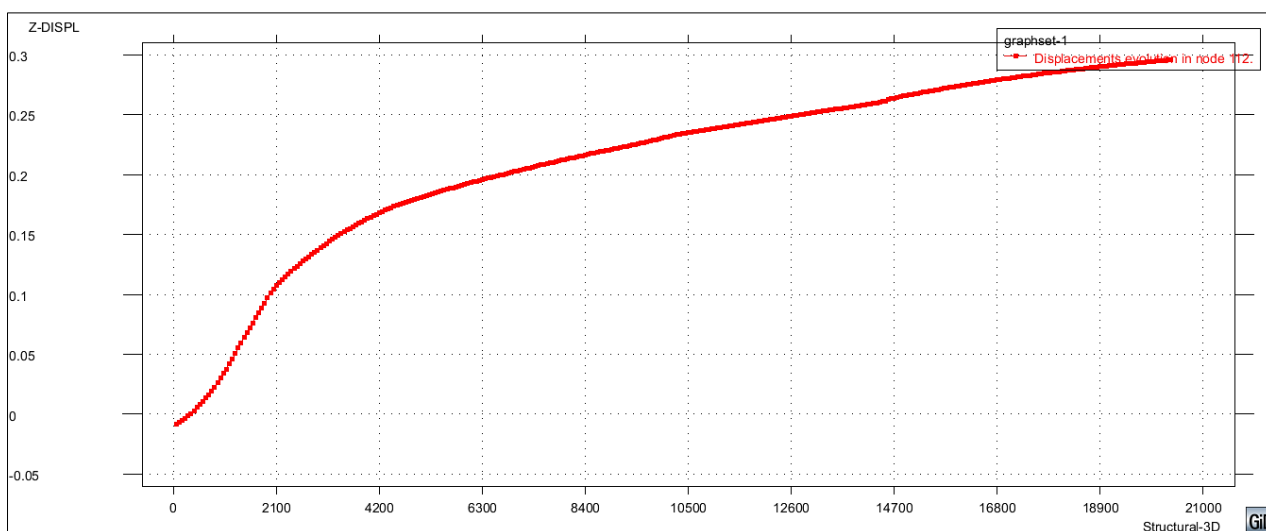


Figure 35. Vertical displacements in the span of axially restrained slabs with span L=5 m exposed to fire from the top

• Bending Moments and Axial Forces in One-Way Simply Supported Slabs with Axial Restraint

Figure 36 shows the bending moments in the longitudinal direction, revealing a notable difference in the diagrams of these moments. The bending moment envelope is observed during the first 30 minutes of fire exposure. Starting from a maximum sagging moment of 24.00 kNm at the mid-span, the moment changes sign and decreases to a hogging moment of 41.10 kNm after 30 minutes. This change in sign is due to the increased stiffness of the slab. As the temperature increases through the depth of the slab, the modulus of elasticity of the material decreases, causing the bending moments to stabilize at nearly constant values after the second hour of fire exposure.

Figure 37 shows a significant change in the normal force over time. At the start of the fire, the normal force is zero. However, as the fire progresses and longitudinal expansion is restricted, a large compressive membrane force develops. The peak compressive membrane force occurs within the first 30 minutes, reaching -720 kN/m. As the fire progresses and the temperature spreads deeper into the slab, after the second hour of fire exposure, the distribution of membrane forces remains almost constant, with compression forces continuing in the middle of the slab. These compressive forces contribute to slab failure as the concrete weakens due to increasing temperature.

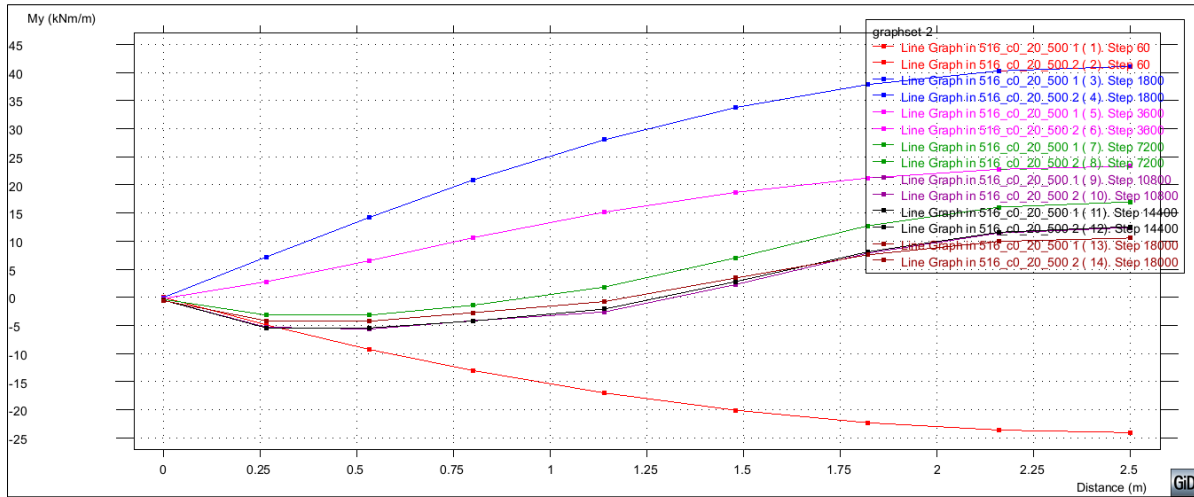


Figure 36. Bending moments (kNm/m) in the longitudinal direction on one-way simply supported slabs axially restrained

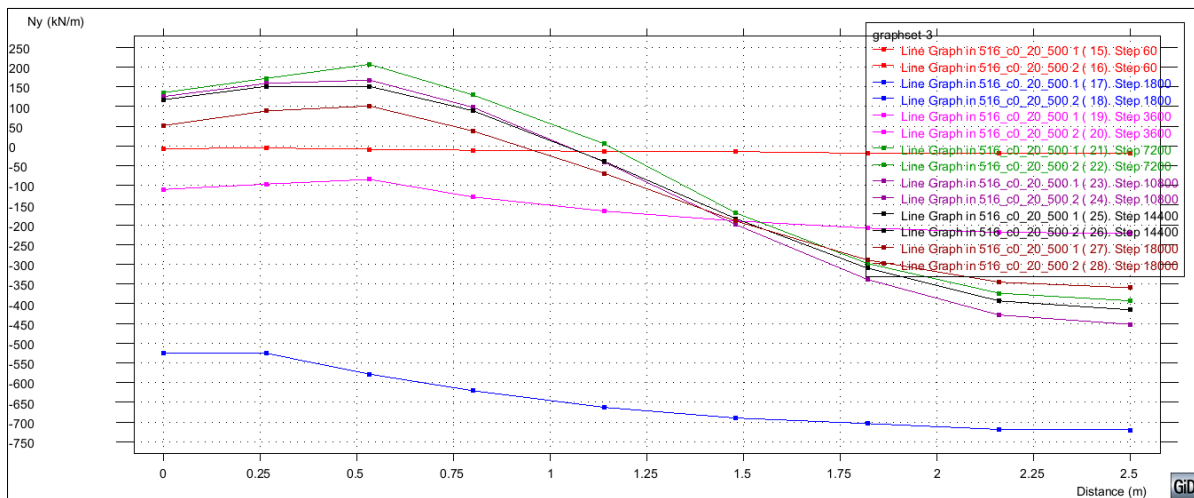


Figure 37. Membrane forces (kN/m) in the longitudinal direction on one-way simply supported slabs axially restrained

• Concrete and Reinforcement Stresses in One-Way Simply Supported Slabs with Axial Restraints

When axial expansion is prevented, the generated axial compressive forces increase the compressive stress in the upper heated zone, where both the external load and temperature contribute to the compressive stress (Figure 38). This results in the crushing of the concrete, which, owing to the high temperatures, has a reduced compressive strength. As a result, the slab fractures much earlier than in a scenario without axial expansion. In these cases, the main reinforcement remains at a relatively low temperature. When the slab fails after 339 minutes, the temperature of the reinforcement reaches 271.5°C, at which temperature the strength of the reinforcement is not significantly reduced. Given that axial expansion is prevented, the reinforcement remains in compression until the slab reaches the point of failure (Figure 39).

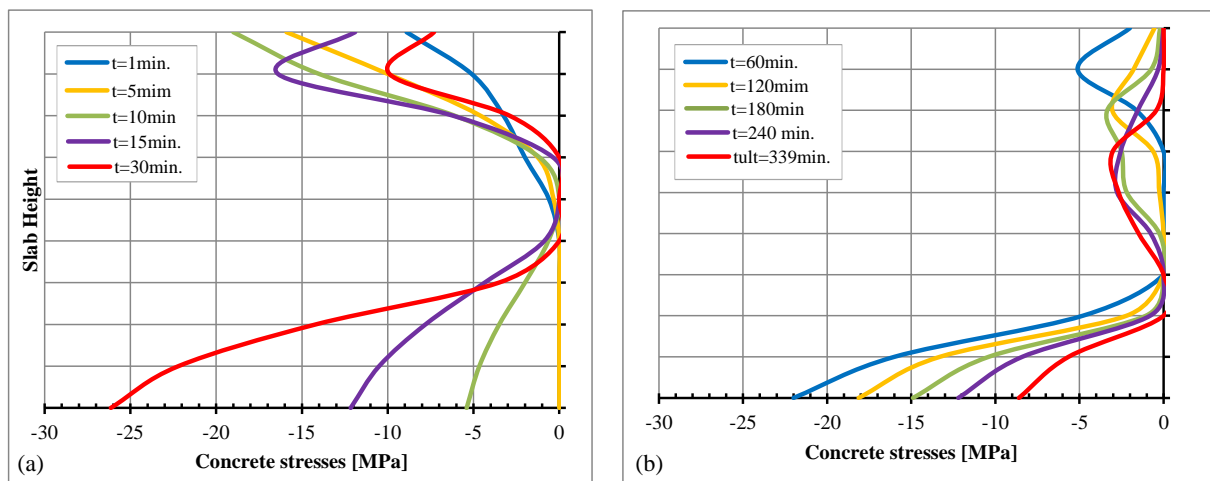


Figure 38. Evolution of concrete stresses over time in the slab cross-section at midspan: a) In the first 30 minutes; b) From the first hour to the sixth hour

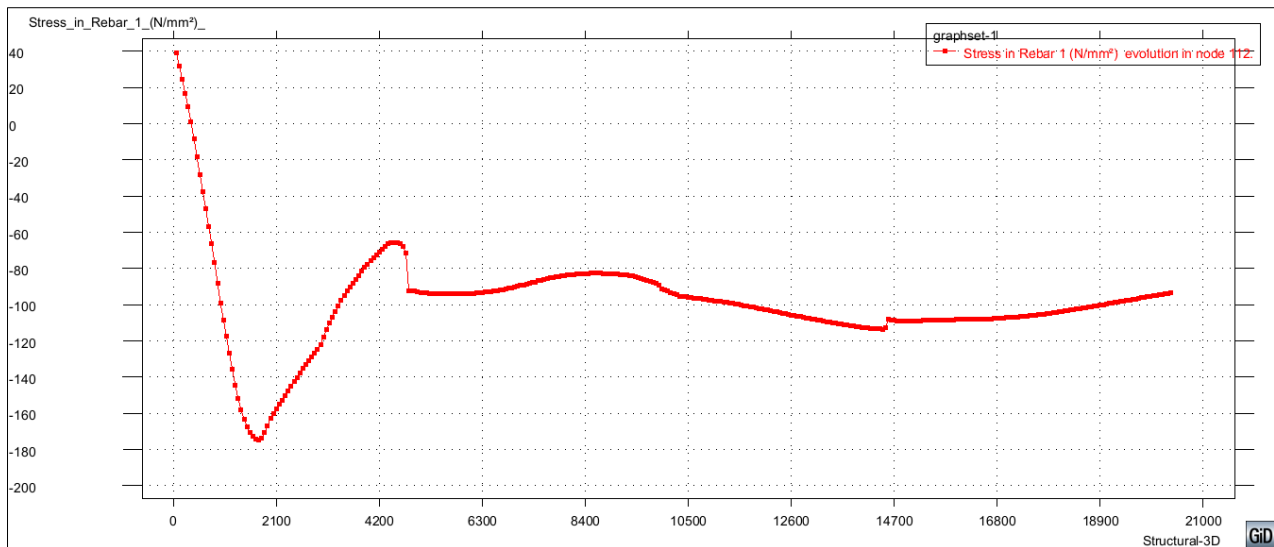


Figure 39. Time evolution of the stresses in the reinforcement at the midspan in a simply supported slab with a span $L=5$ m, with axial restraint, 3D analysis

5.2.3. Comparison of the Fire Resistance between One-Way Simply Supported Slabs without Axial Restraint and those With Full Axial Restraint Exposed to Fire from the Top

Figure 40 shows the vertical midspan displacements of slabs up to failure when exposed to fire from above, comparing two scenarios: axially unrestrained and fully axially restrained slabs. The graph indicates that, unlike cases where fire is applied from below on simply supported slabs, the axially unrestrained slabs demonstrate greater resistance, lasting more than 10 hours, whereas the fully axially restrained slabs fail after 339 minutes.

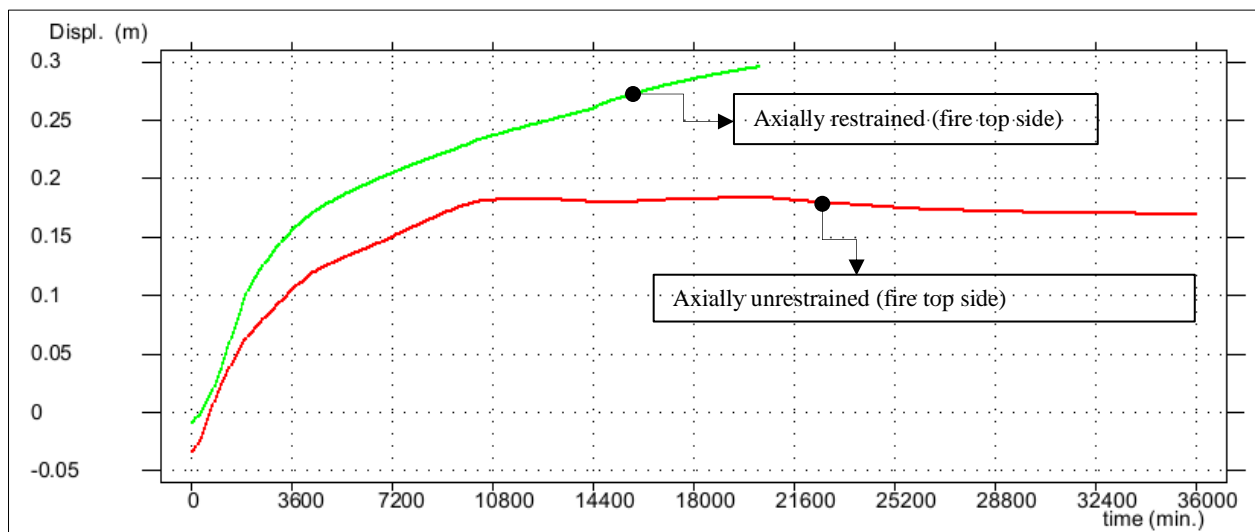


Figure 40. A comparison of vertical displacements at the midspan of slabs with a span of $L = 5$ m, both axially restrained and axially unrestrained, exposed to fire from the top

5.3. Comparison of the Fire Resistance Between One-Way Simply Supported Slabs without Axial Restraint and Those with Full Axial Restraint in Different Fire Scenarios

Figure 41 compares the displacements of a one-way load-bearing slab with a span of $L=5$ m and a concrete cover thickness of 2 cm, which is axially unrestrained and fully axially restrained. It is clear that preventing axial expansion reduces the fire resistance of the slabs when they are exposed to fire from the top, whereas this effect is not observed when the fire acts from the bottom.

In the case of axially unrestrained slabs exposed to fire from above, the slabs exhibit high fire resistance because the main reinforcement is positioned at the bottom, away from the high temperatures impacting the top fibers of the slab. Additionally, in this scenario, large compressive membrane forces are not generated, preventing the concrete from being crushed in the fibers due to the high temperatures.

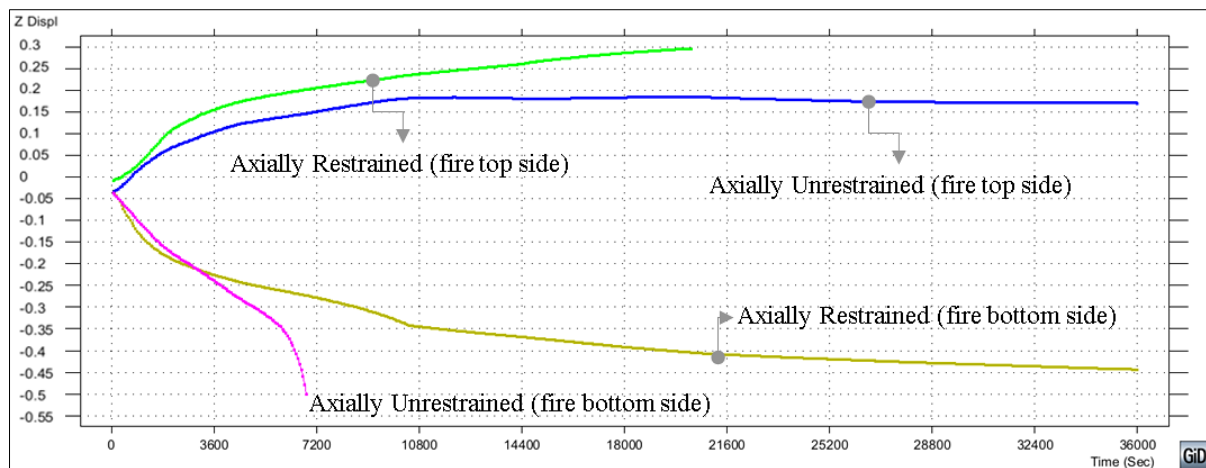


Figure 41. A comparison of vertical displacements at the midspan of slabs with a span of L = 5 m, both axially restrained and axially unrestrained, under different fire scenarios, as obtained through 3D analysis

Salihu et al. [25] demonstrated that the fire resistance of simply supported, axially unrestrained, one-way reinforced concrete slabs with static spans of 4 m, 5 m, and 6 m and a 2 cm concrete cover, calculated via the simplified method outlined in EN 1992-1-2 [17], is 100 minutes. This suggests that design codes are conservative, and to determine the actual fire resistance, a 3-dimensional numerical analysis should be conducted, considering the real conditions the slabs may experience under fire exposure (Table 4).

Table 4. Impact of fire scenario on the fire resistance of one-way simply supported slabs with a span of L = 5 m according to failure criteria

	Fire Resistance (minutes)	
	Fire Bottom	Fire top
Axially Unrestraint	114	>600
Axially Restraint	>600	339

6. Conclusions

The conclusions drawn from this study indicate that implementing these findings in the design of reinforced concrete slabs can substantially improve the fire safety of buildings.

- Simply supported slabs that are axially unrestrained and exposed to fire from the top perform significantly better than those exposed to fire from the bottom, as the main reinforcement remains in the cooler zone. The fire resistance is greater than 10 hours.
- Axial restraint improves the fire resistance of simply supported one-way slabs exposed to fire from the bottom and reduces vertical displacement. This enhancement results from the activation of membrane tension forces along the slab's span and the development of compressive forces in the peripheral regions, creating a ring-like pattern. As a result, the fire resistance exceeds 10 hours.
- When the fire acts from the top, axial restraint reduces the fire resistance of the slabs. The axial compressive forces increase the compressive stress in the upper heated zone, where both external loads and high temperatures contribute to the stress. This leads to crushing of the concrete, which has a reduced compressive strength because of the elevated temperatures. As a result, the slab fractures much earlier than in a scenario without restricted axial expansion. The fire resistance was 339 minutes.
- The lowest fire resistance is observed when the simply supported one-way slab is axially unrestrained, and the fire acts from the bottom, resulting in a fire resistance of 114 minutes.
- The span of one-way, simply supported slabs influences their fire resistance, mainly in terms of allowable deformation. However, this factor is not considered critical in determining the fire resistance of structures, as the primary goal is for the structure to withstand fire for the specified duration of exposure.
- The performance of reinforced concrete slabs under fire conditions is determined mainly by the degree of axial restraint. When analyzed in isolation, it is challenging to precisely predict the extent of the thermal expansion restraint, as this depends on factors such as the slab's location in the structure, the stiffness of adjacent elements, and the fire scenario. Therefore, the most reliable results are obtained when these slabs are analyzed as part of the entire structure.
- The fire resistance calculated via the simplified method outlined in the design code EN 1992-1-2 [17] is 100 minutes, suggesting that the effect of axial restraint is not factored into this calculation.

7. Declarations

7.1. Author Contributions

Conceptualization, F.S., A.G., and M.C.; methodology, F.S., A.G., and M.C.; software, F.S., G.R., and M.C.; validation, F.S., A.G., and F.P.; formal analysis, F.S., A.G., and G.R.; investigation, F.S., A.G., and M.C.; resources, F.S., A.G., and M.C.; data curation, F.S., A.G., and G.R.; writing—original draft preparation, F.S., A.G., and M.C.; writing—review and editing, F.S., A.G., and M.C.; visualization, F.S., A.G., and G.R.; supervision, M.S. and F.P.; project administration, F.S., A.G., and F.P.; funding acquisition, F.S., A.G., G.R., and M.C. All authors have read and agreed to the published version of the manuscript.

7.2. Data Availability Statement

The data presented in this study are available in the article.

7.3. Funding

The authors received no financial support for the research, authorship, and/or publication of this article.

7.4. Conflicts of Interest

The authors declare no conflict of interest.

8. References

- [1] EN 1991-1-2. (2002). Eurocode 1: Actions on structures - Part 1-2: General actions - Actions on structures exposed to fire. The European Union per Regulation 305/2011, Directive 98/34/EC, Directive 2004/18/EC.
- [2] ISO 834. (1975). Fire Resistance Tests, Elements of Building Construction. International Organization for Standardization, Geneva, Switzerland.
- [3] Buchanan, A. H., & Abu, A. K. (2017). Structural design for fire safety. John Wiley & Sons, New Jersey, United States.
- [4] Balaji, A., Nagarajan, P., & Pillai, T. M. (2016). Predicting the response of reinforced concrete slab exposed to fire and validation with IS456 (2000) and Eurocode 2 (2004) provisions. *Alexandria Engineering Journal*, 55(3), 2699-2707. doi:10.1016/j.aej.2016.06.005.
- [5] Bailey, C. G. (2004). Membrane action of slab/beam composite floor systems in fire. *Engineering Structures*, 26(12), 1691-1703. doi:10.1016/j.engstruct.2004.06.006.
- [6] Major, Z., Bodnár, L., Merczel, D. B., Szép, J., & Lublóy, É. (2024). Analysis of the Heating of Steel Structures During Fire Load. *Emerging Science Journal*, 8(1), 1-16.
- [7] Wang, B., Dong, Y. L., & Gao, L. T. (2011). Fire experimental study of four-edge fixed reinforced concrete slab in fire. *Advanced Materials Research*, 163, 1626-1637. doi:10.4028/www.scientific.net/AMR.163-167.1626. doi:10.28991/ESJ-2024-08-01-01.
- [8] Lim, L. C. S., & Wade, C. A. (2002). Experimental fire tests of two-way concrete slabs. *Fire Engineering Research Report 02/12*, University of Canterbury, Christchurch, New Zealand.
- [9] Allam, S. M., Elbakry, H. M., & Rabeai, A. G. (2013). Behavior of one-way reinforced concrete slabs subjected to fire. *Alexandria Engineering Journal*, 52(4), 749-761. doi:10.1016/j.aej.2013.09.004.
- [10] Qiu, P., Duan, J., Yang, Z., Liu, J., & Lu, W. (2024). Research on the Scale Fire Test and Fire Resistance of the One-Way Slab of a Metro. *Buildings*, 14(6), 1695. doi:10.3390/buildings14061695.
- [11] Al-Rousan, R. (2020). Optimum endurance time of reinforced concrete one-way slab subjected to fire. *Procedia Manufacturing*, 44, 520-527. doi:10.1016/j.promfg.2020.02.260.
- [12] Salihu, F., Guri, Z., Cvetkovska, M., & Pillana, F. (2023). Fire Resistance Analysis of Two-Way Reinforced Concrete Slabs. *Civil Engineering Journal (Iran)*, 9(5), 1085-1104. doi:10.28991/CEJ-2023-09-05-05.
- [13] Rasheed, M.R., & Mohammed, S.D. (2024). Structural Behavior of Concrete One-Way Slab with Mixed Reinforcement of Steel and Glass Fiber Polymer Bars under Fire Exposure. *Engineering, Technology & Applied Science Research*, 14(2), 13380-13387. doi:10.48084/etasr.6795.
- [14] Kodur, V., Venkatachari, S., Bhatt, P., Matsagar, V. A., & Singh, S. B. (2023). Fire resistance evaluation of concrete beams and slabs incorporating natural fiber-reinforced polymers. *Polymers*, 15(3), 755. doi:10.3390/polym15030755.
- [15] Elwakkad, N. (2023). Behavior of reinforced self-curing concrete slabs exposed to fire. *Journal of Engineering Sciences*, 51(5), 286-301. doi:10.21608/jesaun.2023.212300.1231.

- [16] Shhabat, M., Ashteyat, A., & Abdel-Jaber, M. (2024). Repairing of One-Way Solid Slab Exposed to Thermal Shock Using CFRP: Experimental and Analytical Study. *Fibers*, 12(2), 18. doi:10.3390/fib12020018
- [17] EN 1992-1-2. (2004). Eurocode 2: Design of concrete structures - Part 1-2: General rules. Structural Fire Design, The European Union Per Regulation 305/2011, Directive 98/34/EC, Directive 2004/18/EC.
- [18] SAFIR (2014). A finite element software for analyzing structures in fire. SAFIR-Computer Program, University of Liege, Liege, Belgium.
- [19] Sanad, A. M., Lamont, S., Usmani, A. S., & Rotter, J. M. (2000). Structural behaviour in fire compartment under different heating regimes—part 2:(slab mean temperatures). *Fire Safety Journal*, 35(2), 117-130. doi:10.1016/S0379-7112(00)00025-4.
- [20] Terro, M. J. (1991). Numerical Modelling of Thermal and Structural Response of Reinforced Concrete Structures in Fire. Imperial College of Science, Technology and Medicine, University of London, London, United Kingdom.
- [21] WFRC. (1987). Ad-Hoc Fire Test Using the Heating Conditions of BS476: Part 8: 1972 on Two 150mm Thick Normal Weight Concrete Slabs. 1987. WARRES No. 40728, Warrington Fire Research Center, (WFRC), London, United Kingdom.
- [22] Cvetkovska, M. (2002). Nonlinear Stress Strain Behaviour of RC Elements and Plane Frame Structures Exposed to Fire. Doctoral Dissertation, Ss Cyril and Methodius University, Skopje, Macedonia.
- [23] Levesque, A. (2006). Fire Performance of Reinforced Concrete Slabs. Master Thesis, Worcester Polytechnic Institute, Worcester, United States.
- [24] Wang, Y., Guo, W., Huang, Z., Long, B., Yuan, G., Shi, W., & Zhang, Y. (2018). Analytical model for predicting the load–deflection curve of post-fire reinforced-concrete slab. *Fire Safety Journal*, 101, 63-83. doi:10.1016/j.firesaf.2018.09.002.
- [25] Salihu, F., & Cvetkovska, M. (2020). Parametric analysis on fire resistance of one way Simply supported reinforced concrete slabs. *International Conference on Contemporary Theory and Practice in Construction XIV STEPGRAD*, 43-54.